Journal of Organometallic Chemistry 977 (2022) 122460

Contents lists available at ScienceDirect

Journal of Organometallic Chemistry

journal homepage: www.elsevier.com/locate/jorganchem

Heterometallic phosphinidene-bridged complexes derived from the phosphanyl complexes *syn*-[MCp(PHR*)(CO)$_2$] (*M* = Mo, W; R* = 2,4,6-$C_6H_2{}^tBu_3$)

M. Angeles Alvarez, M. Esther García, Daniel García-Vivó*, Miguel A. Ruiz*, Patricia Vega

Departamento de Química Orgánica e Inorgánica/IUQOEM, Universidad de Oviedo, E-33071, Oviedo, Spain

ARTICLE INFO

Article history:
Received 29 June 2022
Revised 20 July 2022
Accepted 24 July 2022
Available online 25 July 2022

Keywords:
Heterometallic complexes
Metal-metal bonds
Phosphinidene ligands
Carbonyl ligands
Cyclopentadienyl ligands

ABSTRACT

The title phosphanyl complexes were prepared upon photolysis of equimolar mixtures of dimers [$M_2Cp_2(CO)_6$] and PH_2R^* (R* = 2,4,6-$C_6H_2{}^tBu_3$). They were converted into the corresponding chlorophosphanyl derivatives *syn*-[MCp(PClR*)(CO)$_2$] upon reaction with CCl_4, while its deprotonation (*M* = Mo) yielded the phosphinidene Li[*MoCp*(PR*)(CO)$_2$]. These mononuclear precursors were tested for the synthesis of heterometallic PR*-bridged derivatives by following three synthetic strategies. Photochemical reactions between phosphanyl complexes and dimers [M´$_2$(CO)$_{2n}$] or [M´$_2$Cp$_2$(CO)$_{2n}$] (M' = Mn, Re, Fe, Ru, Co) gave binuclear derivatives of types [MMĆp$_x$(μ-PR*)(CO)$_{n+2}$] and [MoMĆp$_x$(μ-PR*)(CO)$_{n+1}$] (x = 1,2), but yields were very poor except for the WRe complexes. Combinations with Co, Mn, and Re were best made through reaction between carbonylates [M'(CO)$_n$]$^-$ and chlorophosphanyl complexes, to give respectively the pentacarbonyl [MoCoCp(μ-PR*)(CO)$_5$] and the heptacarbonyls [MMĆp(μ-PR*)(CO)$_7$] (MM' = MoRe, MoMn, WMn). The latter were easily decarbonylated thermally to give hexacarbonyls [MMĆp(μ-PR*)(CO)$_6$], which display heterometallic single bonds and short M−P distances of ca. 2.27 Å formulated as double M=P bonds, and rearranged upon thermal or photochemical activation to give the hydride-phosphanyl derivatives [MMĆp(μ-H){μ-P(CH_2CMe_2)$C_6H_2{}^tBu_2$}(CO)$_6$]. This process was suppressed in the photochemical reactions by using a THF/NCMe (10:1) mixture as solvent, but then the acetonitrile complexes [MoMĆp(μ-PR*)(CO)$_5$(1κ-NCMe)] were formed. Combinations with Fe and Ru were best prepared by reacting Li[MoCp(PR*)(CO)$_2$] with halide complexes [MXCp(CO)$_2$], to give the tetracarbonyls [MoMĆp$_2$(μ-PR*)(CO)$_4$] (M' = Fe, Ru), a method also useful to prepare the gold complex [MoAuCp(μ-PR*)(CO)$_2${P(*p*-tol)$_3$}] upon reaction with [AuCl{P(*p*-tol)$_3$}]. The above tetracarbonyl complexes were decarbonylated photochemically to give the metal-metal bound tricarbonyls [MoMĆp$_2$(μ-PR*)(CO)$_3$].

1. Introduction

Phosphinidenes (PR) are very versatile ligands that can coordinate to one or several transition-metal atoms in many different ways [1]. When bound to one or two metal atoms, seven extreme coordination modes have been recognized to date for these ligands, depending on whether the local geometry around the P atom is linear, bent, trigonal or pyramidal, and whether π(M−P) bonding interactions are involved (or not), be them localized or delocalized over the M−P−M skeletons of the corresponding complexes (Chart 1) [1,2]. Because of the low coordination environment for the P atom in all cases, and the presence of lone electron pairs or/and M−P multiple bonding, it can be anticipated that the corresponding complexes would be very reactive towards a great variety of molecules. Indeed, extensive work on the chemistry of bent phosphinidene complexes (of type **B**, usually denoted as *electrophilic*, and **C**, or *nucleophilic* ones) has shown that a great variety of organic reagents can add easily to the M−PR site of these molecules, whereby a large number of unusual organophosphorus ligands can be built on the coordination sphere of the metal atoms [3]. Moreover, detailed work from our lab and others has shown that binuclear complexes with bridging PR ligands, in their different coordination modes (**D** to **G**), are also able to react with a great variety of organic and inorganic compounds to build new

* Corresponding authors.
E-mail addresses: garciavdaniel@uniovi.es (D. García-Vivó), mara@uniovi.es (M.A. Ruiz).

https://doi.org/10.1016/j.jorganchem.2022.122460

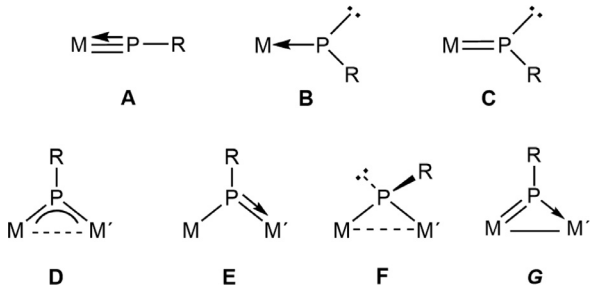

Chart 1. Coordination modes of PR ligands at mono- and binuclear complexes.

organophosphorus ligands and polymetallic derivatives [1a,b, 2]. Most of this previous work, however, has been carried out on homometallic complexes, and little is known about the cooperative and synergic effects that the combination of distinct metal atoms with different coordination environments, as found in *heterometallic* complexes [4], can induce in the case of phosphinidene-bridged complexes.

Detailed studies on the chemical behavior of heterometallic PR-bridged complexes obviously require the implementation of useful synthetic routes for such molecules, which currently are scarce and of limited use or efficiency, and may involve binuclear or mononuclear precursors. Reactions used to build heterometallic PR-bridged complexes from binuclear precursors include deprotonation of a PHR-bridged WFe precursor [5], P–C cleavage in a P(OR)Cp*-bridged MnFe precursor [6], and reactions of thiophosphinidene-bridged Mo_2 complexes with $[Co_2(CO)_8]$ and $[Mn_2(CO)_{10}]$, the latter being of poor selectivity [7,8].

The use of suitable mononuclear phosphanyl precursors, however, might offer superior potential for the synthesis of binuclear heterometallic derivatives, as they could likely lead to more varied combinations of metal atoms. Carty et al. reported the photochemical reactions of a chlorophosphanyl Mo complex with different carbonyl dimers to yield new PR-bridged MoMn and MoCo complexes, following from the homolytic cleavage of a P–Cl bond (method I in Scheme 1) [9], while Schmitt used a two-step sequence (deprotonation and reaction with $[FeClCp(CO)_2]$) to prepare a novel heterometallic WFe complex starting from the phosphanyl precursor $[WCp(PHR^*)(CO)_2]$ (method II; $R^* = 2,4,6\text{-}C_6H_2{}^tBu_3$) [10]. In our preliminary work on this chemistry, we expanded the synthetic toolbox relying on mononuclear phosphanyl complexes by preparing new MoRe complexes through the photochemical reaction of the novel complex *syn*-$[MoCp(PHR^*)(CO)_2]$ (**1a**) with $[Re_2(CO)_{10}]$, this involving P–H and M–M bond homolysis (method III) [11], and through chloride displacement in the chlorophosphanyl derivative *syn*-$[MoCp(PClR^*)(CO)_2]$ (**2a**) by the $[Re(CO)_5]^-$ anion (method IV), with the latter method giving much better yield for the heterometallic complex [2]. This enabled us to widely explore the chemical behavior of $[MoRe(\mu\text{-}PR^*)(CO)_6]$, the first recognized example of a complex of type **G**, a molecule displaying both nucleophilic-like and electrophilic-like structural and chemical features. In this paper we report full studies aimed at establishing the scope of methods II to IV to prepare novel heterometallic complexes by using the phosphanyl complex **1a** or its tungsten analogue *syn*-$[WCp(PHR^*)(CO)_2]$ (**1b**) as primary precursors. As a result, we have been able to efficiently prepare novel heterometallic complexes combining Mo or W atoms with either Re, Mn, Fe, Ru, Co, and Au atoms, many of them displaying the novel coordination mode **G** of its phosphinidene ligand, which involves a P=M double bond to one metal atom and a P→M' donor single bond to the other one.

2. Results and discussion

2.1. Synthesis and structure of mononuclear precursors

In our preliminary work on this chemistry we reported a novel, one-step procedure giving good yields (ca. 70%) of the phosphanyl molybdenum complex **1a**, based on the photochemical reaction of the commercially available dimer $[Mo_2Cp_2(CO)_6]$ with stoichiometric amounts of the primary phosphine PH_2R^* ($R^* = 2,4,6\text{-}C_6H_2{}^tBu_3$) [11]. This reaction likely relies on the photochemically-induced formation of $MoCp(CO)_3$ radicals, a well-established process itself [12], which would initiate chain reactions resulting in P–H bond cleavage in the phosphine to eventually give, after radical coupling and decarbonylation, a mixture of **1a** and the known hydride $[MoCpH(CO)_3]$ [13], as major products Eqs. (1) to (4). We have now found that the tungsten dimer $[W_2Cp_2(CO)_6]$ reacts similarly with PH_2R^* to give the phosphanyl complex *syn*-$[WCp(PHR^*)(CO)_2]$ (**1b**), which can be isolated in ca. 60% yield after chromatographic workup (Scheme 2).

$$M_2Cp_2(CO)_6 + h\nu \rightarrow 2\ \cdot MCp(CO)_3 \quad (1)$$

$$\cdot MCp(CO)_3 + PH_2R^* \rightarrow HMCp(CO)_3 + \cdot PHR^* \quad (2)$$

$$\cdot MCp(CO)_3 + \cdot PHR^* \rightarrow MCp(PHR^*)(CO)_3 \quad (3)$$

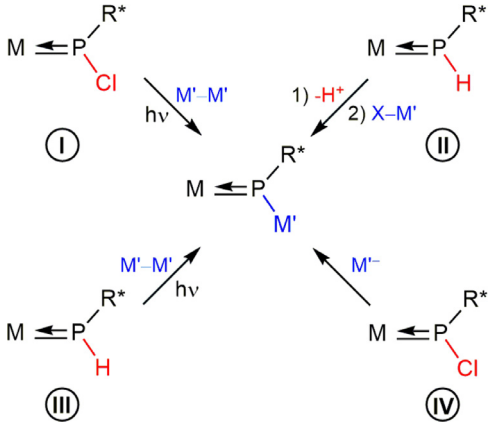

Scheme 1. Synthetic approaches to heterometallic phosphinidene complexes starting from mononuclear phosphanyl complexes.

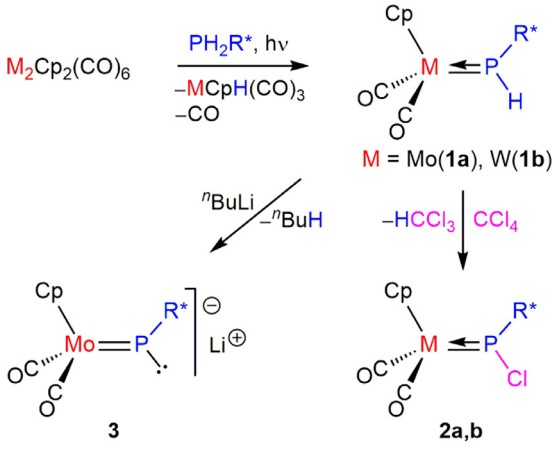

Scheme 2. Preparation of compounds **1**–**3**.

Table 1
Selected IR and $^{31}P\{^1H\}$ NMR data for new compounds.

Compound[a]	ν(CO)	δ (P)
syn-[MoCp(PHR*)(CO)$_2$] (**1a**)[b]	1944 (vs), 1861 (s)	272.7
syn-[WCp(PHR*)(CO)$_2$] (**1b**)	1935(vs), 1850(s)	219.5(623)
syn-[MoCp(PClR*)(CO)$_2$] (**2a**)[c]	1964 (vs), 1892 (s)	266.8
syn-[WCp(PClR*)(CO)$_2$] (**2b**)	1960(vs), 1889(s)[d]	202.9(674)[d]
Li[MoCp(PR*)(CO)$_2$] (**3**)[b]	undetected	1009.5[e]
[MoReCp(μ-PR*)(CO)$_7$] (**4a**)[b]	2135 (m), 2031 (vs), 2002 (m), 1905(w), 1820 (w)	437.6
[MoMnCp(μ-PR*)(CO)$_7$] (**4b**)	2111 (m), 2027 (vs), 2008 (m), 1926 (m), 1831 (m)	458.5(br)
[WReCp(μ-PR*)(CO)$_7$] (**4c**)	2136 (m), 2033 (vs), 2001 (m), 1896 (m), 1811 (m)	329.7(br)
[WMnCp(μ-PR*)(CO)$_7$] (**4d**)	2111 (m), 2027 (vs), 2011 (m), 1919 (m), 1821 (m)	345.3(br)
[MoReCp(μ-PR*)(CO)$_6$] (**5a**)[b]	2077 (m), 1986 (vs), 1951(s), 1876 (w)	673.1
[MoMnCp(μ-PR*)(CO)$_6$] (**5b**)	2055 (m), 2039 (w), 1974 (vs), 1951(s), 1862 (w), 1888 (w)	720.9
[WReCp(μ-PR*)(CO)$_6$] (**5c**)	2076 (m), 1986 (vs), 1946 (s), 1868 (w)	562.5(358)
[WMnCp(μ-PR*)(CO)$_6$] (**5d**)	2054 (s), 1973 (vs), 1948 (s), 1878 (w)	610.7(br)
[MoReCp(μ-H){μ-P(CH$_2$CMe$_2$)C$_6$H$_2$^{t}Bu$_2$}(CO)$_6$] (**6a**)[c]	2086 (m), 1993 (s), 1979 (s), 1954 (vs), 1880 (m)	84.0
[MoMnCp(μ-H){μ-P(CH$_2$CMe$_2$)C$_6$H$_2$^{t}Bu$_2$}(CO)$_6$] (**6b**)	2067 (m), 1993 (m), 1972 (s), 1955 (vs), 1881 (m)	149.2(br)
[WReCp(μ-H){μ-P(CH$_2$CMe$_2$)C$_6$H$_2$^{t}Bu$_2$}(CO)$_6$] (**6c**)	2087 (m), 1995 (s), 1979 (s), 1950 (vs), 1867 (m)	40.8
[MoCoCp(μ-PR*)(CO)$_5$] (**7**)[f]	2031(s), 1972(s), 1958(vs), 1910(w, br)	653.7(br)
[MoFeCp$_2$(μ-PR*)(CO)$_4$] (**8e**)[b]	2027 (s), 1981 (s), 1901 (vs), 1817(s)	477.6
[MoRuCp$_2$(μ-PR*)(CO)$_4$] (**8f**)	2039 (s), 1988 (s), 1901 (vs), 1816 (s)	452.3
[MoFeCp$_2$(μ-PR*)(CO)$_3$] (**9e**)[b]	1945 (m), 1910 (vs), 1770 (m, sh), 1747 (m)	674.0
[MoRuCp$_2$(μ-PR*)(CO)$_3$] (**9f**)	1949 (m, sh), 1938 (m), 1911 (vs), 1734 (m), 1730 (m)	602.0
[MoAuCp(μ-PR*)(CO)$_2${P(*p*-tol)$_3$}][b] (**10**)	1904 (vs), 1817 (s)	528.5
[MoReCp(μ-PR*)(CO)$_5$(1κ-NCMe)] (**11a**)	2062 (m), 1968 (vs), 1956 (s, sh), 1923 (m), 1751 (w)	519.9
[MoMnCp(μ-PR*)(CO)$_5$(1κ-NCMe)] (**11b**)	2034 (w), 2013 (s), 1926 (vs), 1900 (vs)	616.1(br)

[a] IR spectra recorded in dichloromethane solution, unless otherwise stated; NMR spectra recorded in CD_2Cl_2 solution at 121.48 MHz and 293 K, unless otherwise stated, with chemical shifts (δ) in ppm relative to external 85% aqueous H_3PO_4, and ^{31}P-^{183}W couplings (J) in hertz indicated between parentheses.
[b] Data taken from reference 11.
[c] Data taken from reference 2.
[d] IR data in toluene solution; NMR data in C_6D_6 solution. [e] In tetrahydrofuran-d_8 solution. [f] Data taken from reference 7.

$$MCp(PHR^*)(CO)_3 + h\nu \rightarrow MCp(PHR^*)(CO)_2 + CO \quad (4)$$

The *anti* isomers of compounds **1a,b** were previously prepared by Malisch et al. by following several multistep procedures, some of them involving a thermal decarbonylation of the tricarbonyl intermediates MCp(PHR*)(CO)$_3$ appearing in Eq. (4) [14]. Thus, the *syn* conformation of Cp and R* groups around the M=P double bond found for compounds **1a,b**, as confirmed by the observation of positive NOE enhancements between the Cp and *ortho* ^{t}Bu groups in the NOESY spectra of both compounds, might be a consequence of the photochemical (instead of thermal) conditions under which the final decarbonylation step (Eq. (4)) takes place in our case.

Spectroscopic data for compounds **1a,b** (Table 1 and Experimental section) are similar, but not identical, to the ones previously reported for their *anti* isomers in the same solvent. Particularly significant differences are found for the proton PH resonances in C_6D_6 solution, which appear as doublets at 10.20 (J_{PH} = 314 Hz) and 12.52 ppm (J_{PH} = 367 Hz) for compounds **1a** and **1b** respectively, to be compared with 9.95 (J_{PH} = 408 Hz) and 12.8 ppm (J_{PH} = 379 Hz) reported respectively for their *anti* isomers [14]. The tungsten isomers also differ significantly from each other in the corresponding PW coupling, which is 630 Hz for **1b** and 604 Hz for its *anti* isomer. Previous DFT calculations on several tungsten complexes of type [WCp(PHR)(CO)$_2$] revealed that the energies of *syn* and *anti* isomers in this family of molecules are quite similar to each other, with the *anti* conformation being slightly more favored over the *syn* conformation when R = ^{t}Bu, 2,4,6-C$_6$H$_2$Me$_3$, Ph, while the reverse situation holds for the bulkier 2,4,6-C$_6$H$_2$^{t}Bu$_3$ (R*) substituent [10]. However, because of the double-bond nature of the M−P interaction in these complexes, no easy interconversion between *syn* and *anti* isomers is expected in any case, which thus can justify the formation of different isomers (irrespective of their relative thermodynamic stability) when using different synthetic approaches (particularly thermal vs. photochemical procedures) [15].

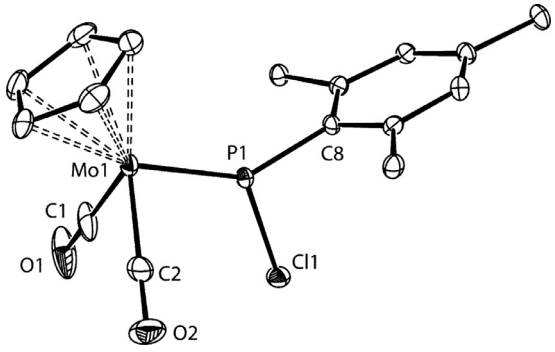

Fig. 1. ORTEP diagram (30% probability) of compound **2a**, with ^{t}Bu (except their C^1 atoms) and H atoms omitted for clarity [2]. Selected bond lengths (Å) and angles (°): Mo−*P* = 2.2212(8); Mo−C1 = 1.975(4); Mo−C2 = 1.952(4); P−Cl = 2.095(1); P − C8 = 1.832(3). Mo−*P* − C8 = 140.1(1); Mo−*P*−Cl = 121.99(4); Cl−P − C8 = 97.8(1); Cl−Mo1−C2 = 83.6(2).

The chlorophosphanyl complexes *syn*-[MCp(PClR*)(CO)$_2$] (*M* = Mo (**2a**), W (**2b**)) can be prepared almost quantitatively through the reaction of compounds **1a,b** with CCl_4, in a process taking place smoothly within a few minutes at room temperature (Scheme 2). Although these complexes decompose upon chromatographic workup, they can be isolated as pure solids through crystallization. However, for most purposes they can be used in further reactions as crude reaction products obtained in situ without any purification and assuming a 100% yield in their formation.

The crystal structure of the molybdenum complex **2a** was determined during our preliminary work on this chemistry [2], which confirmed the retention of the *syn* arrangement of Cp and R* groups around the double Mo=*P* bond of the molecule (Fig. 1), also verified in solution through a standard NOESY experiment. The MoPCl plane almost perfectly bisects the MoCp(CO)$_2$ fragment, as found in the related fluorophosphanyl complex

[MoCp(PFR*)(CO)$_2$] [16], which enables optimum π overlap between the metal and P orbitals to achieve a strong double bond interaction. This is reflected in the short Mo–P length of 2.2212(8) Å, only marginally above the one measured in its fluorophosphanyl analogue (2.204(1) Å), and comparable to the one measured in the chlorophosphanyl complex [MoCp{PCl(TMP)}(CO)$_2$] (2.214(2) Å) which, however, displays an *anti* arrangement of the TMP and Cp ligands around its Mo=P double bond [17].

Spectroscopic data for compounds **2a,b** in solution (Table 1 and Experimental section) are similar, but again slightly different, from the ones reported by Malisch et al. for their *syn* isomers [14]. Besides, they are comparable to each other and to those of the parent compounds **1a,b**, with the expected differences derived from the H/Cl and Mo/W replacements. Thus, their IR spectra display in each case two strong C–O stretching bands some 20–40 cm^{-1} higher than those of the corresponding parent compounds, while bands for the tungsten complexes are somewhat lower than the ones for the Mo complexes. The more energetic band in all cases (symmetric C–O stretch) is slightly more intense than the less energetic one (antisymmetric stretch), which is indicative of a C–M–C angle slightly below 90° in all these compounds (cf. 83.6(2)° for **2a** in the crystal) [18]. In addition, we note that the P W coupling in **2b** (674 Hz) is substantially higher than the one in **1b** (623 Hz), as expected from the higher electronegativity of the P-bound chlorine atom, when compared to hydrogen [19,20].

Previous work by the group of Malisch revealed that the P-bound H atom of the *anti* isomer of **1b** could be removed upon reaction with strong bases such as K(O^{t}Bu) or ^{n}BuLi, to give an anionic phosphinidene species (δ_P 861.4 ppm) which could be easily alkylated or metallated upon reaction with suitable alkyl halides or metal halide complexes [10,14]. The molybdenum complex **1a** behaves similarly, and yields rapidly the anionic phosphinidene complex Li[MoCp(PR)(CO)$_2$] (**3**) upon reaction with ^{n}BuLi in tetrahydrofuran solution at low temperature (Scheme 2). This dark green complex is stable in solution at room temperature for several days, but is extremely air-sensitive, and all attempts to record its IR spectrum only gave C–O stretching bands of the parent compound **1a**. However, full conversion of **1a** into **3** could be verified by recording the ^{31}P NMR spectrum of the reaction mixture following addition of ^{n}BuLi, which only displayed a strongly deshielded resonance at 1009.5 ppm, denoting the quantitative formation of a phosphinidene complex. Presumably, the *syn* stereochemistry of **1a** is retained upon formation of **3**, since its gold derivative (compound **10**) retains a *syn* arrangement of Cp and R* groups around the corresponding Mo=P double bond, as it will be discussed later on.

2.2. Heterometallic derivatives with manganese and rhenium

In our preliminary experiments on this chemistry we found that photolysis of equimolar amounts of **1a** and [Re$_2$(CO)$_{10}$] gave the MoRe compound [MoReCp(μ-PR*)(CO)$_7$] (**4a**) in moderate yield (method III in Scheme 1), along with some [MoReCp(μ-PR*)(CO)$_6$] (**5a**) and its isomer [MoReCp(μ-H){μ-P(CH$_2$CMe$_2$)C$_6$H$_2$^{t}Bu$_2$}(CO)$_6$] (**6a**). Separate experiments revealed that **4a** could be decarbonylated thermally to give the metal-metal bound **5a**, while the latter could be transformed into its phosphanyl isomer **6a** upon strong heating or prolonged photolysis [2,11]. However, compound **4a** could be prepared much more efficiently through the reaction of the carbonylate Na[Re(CO)$_5$] with the chlorophosphanyl complex **2a** (method IV in Scheme 1) [2]. In contrast, we found that the opposite method II, that is, the one based on the reaction of the anionic phosphinidene complex **3** with an halide complex such as [ReBr(CO)$_5$], resulted in net electron transfer eventually producing a mixture of **1a** and [Re$_2$(CO)$_{10}$]. The parent complex in the latter reaction is likely formed through H-atom abstraction from the solvent or traces of water present in it by the resulting radical phosphinidene complex, while rhenium carbonyl would be formed through dimerization of Re(CO)$_5$ radicals Eqs. (5) to (8). We have now examined all the above synthetic strategies as potential routes to prepare analogous complexes bearing MoMn, WRe and WMn dimetal centers.

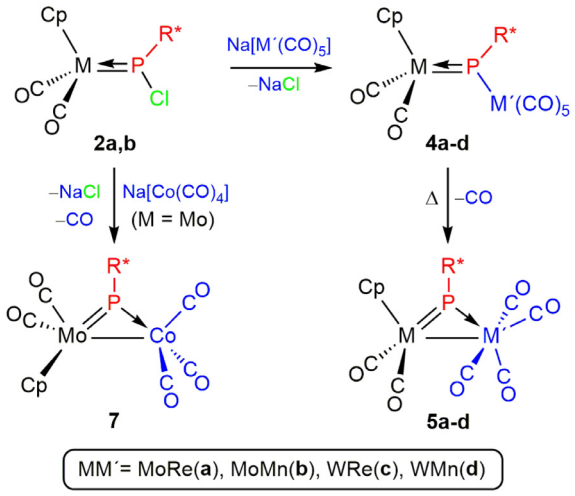

Scheme 3. *Re*, Mn, and Co derivatives of compounds **2**.

$$\mathbf{3} + XM(CO)_5 \rightarrow \cdot MoCp(PR)(CO)_2 + \cdot M(CO)_5X^- \quad (5)$$

$$\cdot M(CO)_5X^- \rightarrow \cdot M(CO)_5 + X^- \quad (6)$$

$$\cdot MoCp(PR)(CO)_2 + \cdot H \rightarrow \mathbf{1a} \quad (7)$$

$$\cdot M(CO)_5 + \cdot M(CO)_5 \rightarrow M_2(CO)_{10} \quad (8)$$

Method II was checked as a route to prepare MoMn and WRe complexes analogous to the MoRe complex **4a**, but the only complexes formed upon reaction of **3** with [MnI(CO)$_5$] were **1a** and [Mn$_2$(CO)$_{10}$], while the reaction between the tungsten analogue of **3** and [ReBr(CO)$_5$] yielded **1b** and [Re$_2$(CO)$_{10}$] as the only organometallic products. This indicates that undesired electron transfer, rather than nucleophilic displacement of halide, is the dominant process in all these cases.

As for the photochemical method III, we found that reactions between the phosphanyl complexes **1a,b** and dimers [M$_2$(CO)$_{10}$] (*M* = Mn, Re) proceeded analogously as the one described above, to give mixtures of compounds of types **4, 5**, and **6** in different proportions. Yet, all of them were of poor efficiency for the preparation of heterometallic phosphinidene complexes of type **4**, with the W/*Re* reaction giving the highest yield (ca. 30% of complex [WReCp(μ-PR*)(CO)$_7$] (**4c**) after chromatographic workup).

Method IV proved to be the preferable method to build most heterometallic complexes of type **4** (Scheme 3). It is particularly selective for the MoMn combination (compound [MoMnCp(μ-PR*)(CO)$_7$] (**4b**)), but not as efficient for the WMn and WRe combinations, since significant amounts of **1b** are formed in these cases, which suggests that the undesired electron transfer is a competitive side reaction for these metal combinations. In any case, the yields of all these products after chromatographic workup were modest, due to their progressive decarbonylation to yield the corresponding hexacarbonyls of type **5**, a process taking place slowly

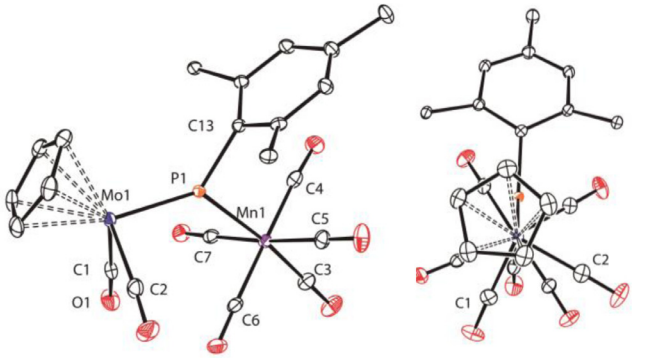

Fig. 2. ORTEP diagram (30% probability) of compound **4b**, with ^{t}Bu (except their C^1 atoms) and H atoms omitted for clarity. On the right, projection of the structure along the Mo–Mn axis.

Table 2
Selected bond lengths (Å) and angles (°) for compound **4b**.

Mo1···Mn1	4.2878(5)	Mo1–P1–Mn1	127.46(3)
Mo1–P1	2.2922(6)	Mo1–P1–C13	130.46(8)
Mn1–P1	2.4884(7)	Mn1–P1–C13	102.08(8)
Mo1–C1	1.941(3)	P1–Mo1–C1	90.35(8)
Mo1–C2	1.958(3)	P1–Mo1–C2	93.86(8)
Mn1–C3	1.839(3)	P1–Mn1–C3	174.4(1)
Mn1–C4	1.860(3)	P1–Mn1–C4	94.46(8)
P1–C13	1.866(2)	C1–Mo1–C2	82.2(1)

even in solution at room temperature, and being promoted by the chromatographic support. As expected, complexes **5** could be conveniently prepared in general by heating the crude reaction mixtures obtained in the above reactions, followed by chromatographic workup (Scheme 3). This yielded the corresponding hexacarbonyls [MM'Cp(μ-PR*)(CO)$_6$] (MM' = MoRe (**5a**), MoMn (**5b**), WRe (**5c**), WMn (**5d**)) in overall yields ranging from 40 to 70%, based on the parent compounds **1a,b** (see the Experimental section). We should note that methods III and IV had never been used for the synthesis of phosphinidene-bridged heterometallic complexes prior to our work.

2.2.1. Structure of the heptacarbonyl complexes 4a-d

The crystal structure of the MoRe complex **4a** was determined in our preliminary work on this chemistry, and the one for its manganese analogue **4b** is similar (Fig. 2 and Table 2). The latter molecule can be derived from that of the chlorophosphanyl complex **2a** by just replacing the chlorine atom with a Mn(CO)$_5$ fragment, which thus acquires a quite regular octahedral environment, while the *syn* conformation of Cp and R* groups around the Mo–P double bond of the molecule is retained. The corresponding Mo–P distance of 2.2922(6) Å, while comparable to the one previously measured for the MoRe complex **4a** (2.3032(9) Å) [11], is significantly longer than expected for a Mo–P double bond (cf. 2.2212(8) Å for **2a**), and actually comparable to the figure of 2.297(8) Å measured for [Mo$_2$Cp$_2$(μ-PR*)(CO)$_4$] [21], a symmetrical complex of type **D** for which a Mo–P bond order of 1.5 should be proposed. Such elongation in **4a** might be thus attributed to some delocalization of the π-bonding interaction over the Mo–*P*–Mn backbone, an effect previously found by us in some heterometallic MoMn and MoCo complexes of type **E** [7,8]. However, this elongation could be also attributed to the steric pressure introduced by the presence of the Mn(CO)$_5$ group (cf. Mo–P = 2.284(4) Å in the sterically congested complex [MoCp(P^{t}Bu$_2$)(CO)$_2$]) [22]. We currently favor the hypothesis of steric effects as the major responsible for the observed elongation in **4a**, based on the fact that the MoPMn plane deviates significantly (by some 20°) from the plane bisecting

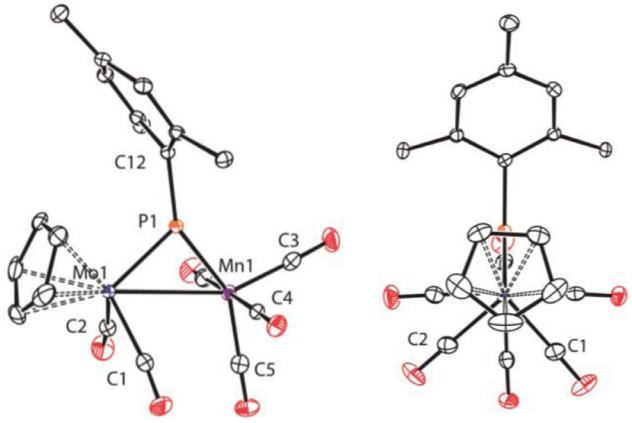

Fig. 3. ORTEP diagram (30% probability) of compound **5b**, with ^{t}Bu (except their C^1 atoms) and H atoms omitted for clarity. On the right, projection of the structure along the Mo–Mn axis.

Table 3
Selected bond lengths (Å) and angles (°) for compound **5b**.

Mo1–Mn1	3.1049(3)	Mo1–P1–Mn1	87.61(2)
Mo1–P1	2.2638(4)	Mo1–P1–C12	123.34(5)
Mn1–P1	2.2214(5)	Mn1–P1–C12	149.03(5)
Mo1–C1	1.996(2)	P1–Mo1–C1	107.07(5)
Mo1–C2	1.981(2)	P1–Mo1–C2	104.51(5)
Mn1–C3	1.794(2)	P1–Mn1–C3	106.62(6)
Mn1–C4	1.866 (2)	P1–Mn1–C4	90.58(5)
Mn1–C5	1.842(2)	P1–Mn1–C5	151.03(6)
P1–C12	1.832(2)	C1–Mo1–C2	85.88(8)

the CpMo(CO)$_2$ fragment (Fig. 2, right), to the detriment of optimal π(Mo–P) bonding. As it will be discussed below, such a rotational distortion is much smaller for the MoAu complex **10**, which accordingly displays a shorter Mo–P distance. In line with this interpretation, the Mn–P distance of 2.4884(7) Å is not particularly short, but actually longer than the reference value of 2.46 Å for a single-bond between these atoms [23], or the value of 2.466(2) Å measured for the diphosphanyl complex [Mn(η^2-P^{t}BuP^{i}Pr$_2$)(CO)$_4$] [24].

Spectroscopic data in solution for compounds **4a-d** (Table 1 and Experimental section) are comparable to each other and essentially consistent with the structures determined in the solid state for the molybdenum complexes **4a,b**. They all show five C–O stretches, with frequencies and relative intensities that denote the presence of essentially independent octahedrally-derived M(CO)$_5$ and cisoid M(CO)$_2$ oscillators, with the expected differences derived from the change in metal (C–O stretching frequencies in the order Mo>*W* and Re>Mn) [18]. The ^{13}C NMR spectra of these compounds display a single resonance for the Mo- or W-bound carbonyls in each case, which denotes the presence of a (real or time-averaged) symmetry plane in solution bisecting the MCp(CO)$_2$ fragment of these molecules, absent in the crystal structures. Their ^{31}P NMR spectra display resonances in the range 330–460 ppm, significantly more deshielded than those of their phosphanyl precursors and with strong influence of the metals there present, with the lighter atoms giving rise to the more deshielded resonances as expected [25].

2.2.2. Structure of hexacarbonyl complexes 5a – d

In our preliminary work on this chemistry, we determined the crystal structures of the rhenium complexes **5a** [2] and **5c** [26]. Because of some differences in the IR spectra to be discussed later on, we also decided to determine the crystal structure of the MoMn complex **5b** (Fig. 3 and Table 3). The latter however turned to be similar to those of the rhenium complexes, also re-

taining the *syn* conformation of the Cp and R* groups around a Mo–P bond of substantial multiplicity, with the metal atoms being further linked through a conventional intermetallic bond (Mo–Mn = 3.1049(3) Å). The MoPMn plane in this complex almost bisects the $MoCp(CO)_2$ fragment, thus allowing for optimal π(Mo–P) bonding. As a result, the Mo–P distance of 2.2638(4) Å in **5b** is slightly shorter than the corresponding distances in the rhenium complexes **5a,c** (ca. 2.273 Å), and approaches the measured lengths of the Mo–P double bonds in trigonal phosphanyl complexes (cf. 2.2212(8) Å in **2a**). On the other hand, the Mn–P distance of 2.2214(4) Å falls in the short edge of the range 2.22–2.37 Å found for dative P→Mn bonds in conventional phosphines bound to Mn in related coordination environments (cf. 2.2266(7) Å for the average length in *axe,axe*-$[Mn_2(CO)_8(PPhC_{12}H_8)_2]$ [27,28]. All these geometrical details, added to the results of our previous DFT calculations on **5a** [2], reinforce our description of the metal-phosphorus bonding in complexes **5** as a new type of interaction (**G** in Chart 1), involving a M=P double bond to one metal, as found in mononuclear nucleophilic complexes, and a P→M dative single bond to the other one, as found in mononuclear electrophilic complexes (Scheme 3). We finally note that a complex similar to **5b**, $[MoMnCp(\mu\text{-}P(TMP)\}(CO)_6]$ (TMP = tetramethylpiperidinyl), was previously reported by Carty et al. by following the photochemical synthetic method I [9]. The geometrical parameters for this complex, however, differ significantly from the ones for **5b**, as it displays a different conformation of the $MoCp(CO)_2$ fragment relative to the MoPMn plane, a longer Mo–P distance (2.2912(5) Å) and a shorter Mn–P distance (2.1862(6) Å), which is consistent with a more delocalized π-bonding interaction over the Mo–P–Mn backbone in this case (type **D** in Chart 1).

In solution, the IR spectra of compounds **5a,c,d** (Table 1) display four C– O stretching bands, with relative intensities indicative of substantial vibrational coupling between the $M(CO)_2$ and $M'(CO)_4$ oscillators of these molecules, while the band at the highest frequency, mostly due to the symmetric stretch of the $M(CO)_4$ fragment, is some 60 cm^{-1} less energetic than the corresponding stretch of the $M(CO)_5$ fragment in compounds **4**, as expected. In contrast, the IR spectrum of the MoMn complex **5b** displays, along with the expected symmetric stretch at 2055 cm^{-1}, an additional high-frequency band of weak intensity at 2039 cm^{-1}. The relative intensity of this band remained constant in all spectra of the complex, even upon dissolving crystalline samples of it. However, such band was absent in the solid-state spectrum of the crystals used in the X-ray study discussed above (see the Experimental section). Thus we conclude that complex **5b** exhibits a second but minor isomer in solution, likely a rotamer (see below), which would be in equilibrium with the major isomer. The interconversion between the isomers of **5b** appears to be fast on the NMR timescale, since all the ^{31}P, ^{1}H or ^{13}C NMR spectra of **5b** failed to detect the presence of more than one species down to 185 K. We finally note that the ^{31}P NMR resonances of compounds **5** fall in the range 563–721 ppm, some 250 ppm above the resonances of the corresponding compounds of type **4,** a deshielding that might be related to the presence of a metal–metal bond in compounds **5**, which is an effect well documented for binuclear phosphanyl-bridged complexes [25]. Other spectroscopic data for compounds **5** are as expected and deserve no additional comments.

2.3. Heterometallic derivatives with cobalt

During a previous study on the reactions of thiophosphinidene-bridged dimolybdenum complexes with $[Co_2(CO)_8]$ we came across the MoCo phosphinidene complex $[MoCoCp(\mu\text{-}PR^*)(CO)_5]$ (**7**) [7], a molecule strongly related to compounds **5**, which might be worthy of further reactivity studies. Unfortunately, the above reactions are rather cumbersome and inefficient as preparative routes to compound **7**. Based on the electronic similarity of **7** with compounds **5** we then attempted its selective synthesis by using the preparative method IV. Indeed, the chlorophosphanyl complex **2a** reacts readily with $K[Co(CO)_4]$ in dichloromethane solution, to give instantaneously a dark green solution of complex **7** (Scheme 3), which can be isolated in ca. 80% after chromatographic workup, thus paving the way for future studies on this heterometallic complex. No intermediates were detected in this fast reaction, which presumably should involve first the formation of the hexacarbonyl intermediate $[MoCoCp(\mu\text{-}PR^*)(CO)_6]$, followed by decarbonylation to yield complex **7**.

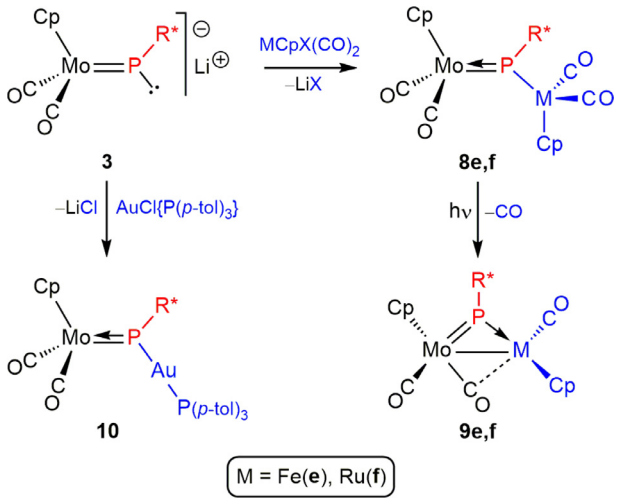

Scheme 4. Fe, Ru and Au derivatives of compound **3**.

The structure of **7** in the crystal revealed that the phosphinidene ligand was more tightly bound to the Mo atom than to the Co one [7]. Indeed, the Mo–P distance of 2.266(2) Å is identical to the one measured in the manganese complex **5b**, and might be viewed as corresponding to a Mo–P double bond. Therefore, rather than classifying complex **7** as one of type **D**, as assumed at the time, we currently favor a description of the phosphinidene-metal interaction in this molecule in terms analogous to complexes **5** (type **G**), with the P atom being involved in an essentially localized double bond to Mo and a donor single bond to Co.

2.4. Heterometallic derivatives with iron and ruthenium

In our preliminary work on this chemistry we found that reaction of the anionic phosphinidene complex **3** with $[FeICp(CO)_2]$ yielded the expected heterometallic derivative $[MoFeCp_2(\mu\text{-}PR^*)(CO)_4]$ (**8e**) in a very selective way (method II), with the latter complex being photochemically decarbonylated to give the metal-metal bound derivative $[MoFeCp_2(\mu\text{-}PR^*)(CO)_3]$ (**9e**) [11]. We have now found that related MoRu complexes can be prepared using this synthetic strategy (Scheme 4), although the first step is not that selective. Reaction of **3** with $[RuBrCp(CO)_2]$ proceeds slowly at room temperature, to give $[MoRuCp_2(\mu\text{-}PR^*)(CO)_4]$ (**8f**) in moderate yield, along with **1a** and $[Ru_2Cp_2(CO)_4]$ as identified side-products. The formation of the latter products indicate that electron-transfer steps comparable to those represented by Eqs. (5) to 8 are competitive with the main reaction, thus reducing significantly the yield of the targeted heterometallic complex. As expected, compound **8f** could be decarbonylated photochemically to give the corresponding metal-metal bound derivative $[MoRuCp_2(\mu\text{-}PR^*)(CO)_3]$ (**9f**) in good yield (Scheme 4). We also checked the photochemical method III as a possible route for these MoRu complexes, but then complex mixtures of products containing only small amounts of **8f** and **9f** were obtained. We finally

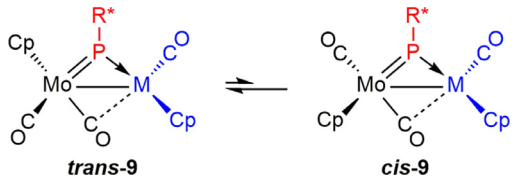

Scheme 5. Proposed isomerism for compounds **9** in solution.

checked the alternative method IV by reacting the chlorophosphanyl complex **2a** with Na[RuCp(CO)$_2$] in tetrahydrofuran. This yielded a mixture of **8f, 1a** and [Ru$_2$Cp$_2$(CO)$_4$], with lower amounts of the MoRu complex (compared to those obtained when using method II), this revealing that the undesired electron transfer now prevails over the nucleophilic displacement of chloride by the ruthenium carbonylate.

Spectroscopic data for compounds **8e,f** are similar to each other and comparable to those previously described for the related tungsten complexes [WFeCp$_2$(μ-PR)(CO)$_4$] (R = 2,4,6-C$_6$H$_2$Me$_3$, 2,4,6-C$_6$H$_2$^{t}Bu$_3$) [5,10], then deserving no detailed comments. We just note that the phosphinidene ligand gives rise to ^{31}P resonances with chemical shifts comparable to that of the MoMn complex **4b**, while the ^{1}H and ^{13}C NMR spectra denote the presence of an effective symmetry plane relating pairs of carbonyl and *ortho*-^{t}Bu groups. Presumably, these complexes retain the *syn* arrangement of Cp and R* groups around the respective Mo–P double bonds.

The IR spectrum of the tricarbonyl complexes **9** display four (**9e**) or five (**9f**) C–O stretches (Table 1), thus suggesting the presence of two isomers in solution in both cases, not detected by the respective NMR spectra at room temperature, which display resonances attributable to a single species in each case. The iron complex displays two low frequency bands at 1770 and 1747 cm^{-1}, while the corresponding bands in the ruthenium complex are less energetic, 1734 and 1730 cm^{-1}. This suggests that the isomers present in solution display bridging or semibridging carbonyls, perhaps with a tighter interaction to the second metal atom in the case of the ruthenium complex [29]. More explicit evidence for the presence of two isomers in solution was obtained from the low-temperature ^{31}P NMR spectra of the iron complex **9e**. Upon cooling, the sharp ^{31}P NMR resonance at 674.0 ppm observed for **9e** at room temperature broadened progressively, to eventually split below 223 K into two broad resonances of different intensity, appearing at 675.1 and 628.5 ppm with relative intensities of ca. 3:1 at 193 K (see the Supplementary material). Taking into account the X-ray determined structure of the tungsten complex analogous to **9e**, which displayed a weak semibridging interaction of one of the W-bound carbonyls to the iron atom (Fe···C = 2.433(3) Å) and a transoid arrangement of the Cp ligands [10], we propose for the major isomer in **9e** a similar transoid arrangement of Cp and terminal CO ligands, while the minor isomer would be the corresponding *cis* isomer, not observed for the tungsten complex (Scheme 5). The ruthenium complex **9f** likely displays a similar isomerism, but in this case no NMR evidence for the presence of two isomers in solution was obtained, since the sharp ^{31}P NMR resonance at 602.0 ppm observed for **9f** at room temperature just broadened progressively upon cooling, with no observable splitting down to 183 K (see the Experimental section).

Attempts to determine the solid-state structure of the iron complex **9e** failed, but we succeeded with the ruthenium complex **9f** (Fig. 4 and Table 4). There are two independent molecules (A and B) in the unit cell. Both of them are made from MCp(CO) fragments arranged in a transoid disposition and connected through an intermetallic single bond (Mo–Ru ca. 2.96 Å), an asymmetrically bridging phosphinidene ligand, and an additional Mo-bound carbonyl involved in a semibridging interaction to the ruthenium

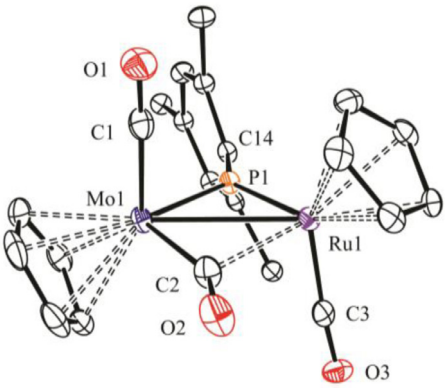

Fig. 4. ORTEP diagram (30% probability) of compound **9f**, with ^{t}Bu (except their C^1 atoms) and H atoms omitted for clarity. Only one (A) of the two independent molecules in the unit cell shown.

Table 4
Selected Bond Lengths (Å) and Angles (°) for Compound 9f[a].

	Mol A	Mol B		Mol A	Mol B
Mo1–Ru1	2.9628(4)	2.9597(4)	Mo1–P1–Ru1	81.71(3)	81.92(3)
Mo1–P1	2.2466(8)	2.250(1)	Mo1–P1–C14	134.2(1)	152.1(1)
Ru1–P1	2.2823(8)	2.265(1)	Ru1–P1–C14	143.8(1)	125.9(1)
Mo1–C1	1.959(4)	1.959(6)	P1–Mo1–C1	94.9(1)	96.4(1)
Mo1–C2	2.032(4)	2.090(5)	P1–Mo1–C2	100.0(1)	96.9(1)
Ru1–C3	1.852(4)	1.887(5)	P1–Ru1–C3	103.5(2)	96.4(1)
Ru1···C2	2.309(4)	2.189(5)	Mo1–C2–O2	152.1(3)	143.1(5)
P1–C14	1.849(3)	1.847(3)	Ru1–Mo1–C2	51.0(1)	47.6(2)

[a] Two independent molecules (A and B) in the unit cell.

atom. The latter interaction seems somewhat stronger for molecule B, as judged from the relevant geometrical parameters [30]: (a) a smaller Mo–C–O angle of 143.1(5)° (vs. 152.1(3)° for molecule A), (b) a longer Mo–CO distance of 2.090(5) Å (vs. 2.032(4) Å), and (c) a shorter Ru···CO separation of 2.189(5) Å (vs 2.309(4) Å). We note that, while both semibridging interactions are definitively stronger than the one identified in the mentioned WFe complex, the differences between those at molecules A and B might be derived from packing forces in the crystal. The different tilting of the R* group toward the Ru atom (Mo–P–C14 = 134.2(1) and 152.1(1)° respectively) might have a similar origin. In contrast to these differences, the M–P distances in both molecules are similar to each other, with a Mo–P separation of ca. 2.25 Å even shorter than those measured for compounds **5**, therefore consistent with the formulation of Mo–P double bonds, while the Ru–P separations of ca. 2.27 Å (significantly longer, if we allow for the ca. 0.08 Å difference in the covalent radii of Mo and Ru) [23], would be consistent with the formulation of donor single bonds (eg. 2.2641(8) Å in the diphosphine complex [MoRuCp$_2$(CO)$_3$(μ-Ph$_2$PCH$_2$PPh$_2$)] [31,32]. At this point we should recall that the tungsten analogue of **9e** also displayed a similarly short W–P separation of 2.2488(8) Å, while the Fe–P separation of 2.1616(9) Å might be consistent with the formulation of a donor single bond too [33]. On all the above considerations, we propose for compounds **9** an electron distribution similar to the one in compounds **5**, that is one involving Mo=P double bonds and P→Fe/Ru donor single bonds (type **G**).

2.5. Heterometallic derivatives with gold

In our preliminary work on this chemistry we found that reaction of the Na$^+$ salt of the radical phosphanyl anion [MoCp(PHR)(CO)$_2$]$^-$ with [AuCl{P(*p*-tol)$_3$}] gave the heterometallic phosphinidene derivative [MoAuCp(μ-PR*)(CO)$_2${P(*p*-tol)$_3$}] (**10**), although the yield was rather modest [11]. We have now tested method II as a way to improve the preparation of this phos-

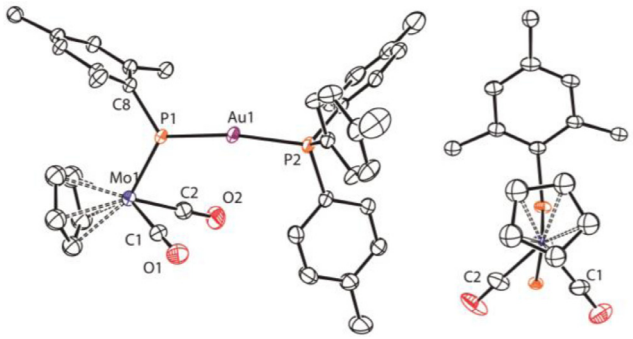

Fig. 5. ORTEP diagram (30% probability) of compound **10**, with ^{t}Bu (except their C^1 atoms) and H atoms omitted for clarity. On the right, projection of the structure along the Mo···Au axis, with *p*-tol rings omitted.

Table 5
Selected bond lengths (Å) and angles (°) for compound 10.

Mo1···Au1	4.0173(5)	Mo1–P1–Au1	123.10(4)
Mo1–P1	2.264(1)	Mo1–P1–C8	116.1(1)
Au1–P1	2.305(1)	Au1–P1–C8	120.6(1)
Mo1–C1	1.940(5)	P1–Mo1–C1	89.3(2)
Mo1–C2	1.948(5)	P1–Mo1–C2	87.2 (2)
Au1–P2	2.296(1)	P1–Au1–P2	168.14(3)
P1–C8	1.854(3)	C1–Mo1–C2	79.5(2)

phinidene complex, and have also determined its crystal structure (Fig. 5 and Table 5). Indeed, complex **10** can be more efficiently prepared (60% yield) by reacting the anionic phosphinidene complex **3** with [AuCl{P(*p*-tol)$_3$}] in tetrahydrofuran solution (Scheme 4).

The structure of **10** can be derived from that of **2a** but just replacing the chlorine atom with the Au(*p*-tol)$_3$ fragment, with retention of the *syn* conformation of Cp and R* groups around the Mo–P multiple bond of the molecule. The coordination environment for the gold atom is essentially linear as expected (P1–Au1–P2 = 168.14(3)°), with Au–P distances almost identical to each other (ca. 2.30 Å). On the other hand, the Mo–P distance of 2.264(1) Å is identical to the one measured for the manganese compound **5b**, and consistent with the Mo–P double bond to be formulated for this complex on electron counting grounds. Such a distance, however, is significantly shorter than the ones measured for compounds **4a,b** (ca. 2.30 Å), for which Mo–P double bonds should be also formulated according to the usual electron counting scheme. This reinforces our view, already noted above, than the unusual lengthening in the Mo–P bonds of compounds **4a,b** are due to the steric pressure introduced by the space-demanding M(CO)$_5$ fragment of these molecules, much diminished in the case of the gold complex thanks to its lineal coordination environment. Moreover, we also note that the Mo–P–Au plane in **10** is close to the ideal plane bisecting the MoCp(CO)$_2$ fragment, thus allowing for optimum π overlap between Mo and P orbitals, therefore for a stronger Mo–P bond.

2.6. Thermal and photochemical reactions of hexacarbonyl complexes 5

Previous studies on the dimolybdenum complex [Mo$_2$Cp$_2$(μ-PR*)(CO)$_4$] revealed that, upon thermal or photochemical activation, this complex could undergo a number of interesting processes including coordination of the aryl ring, C–H activation of the Cp ligands and formation of Mo–Mo triple bonds following decarbonylation, as well as isomerization involving C–H activation of the ^{t}Bu groups in the PR* ligand [34,35]. With this chemistry in mind we then examined the thermal and photochemical reactions

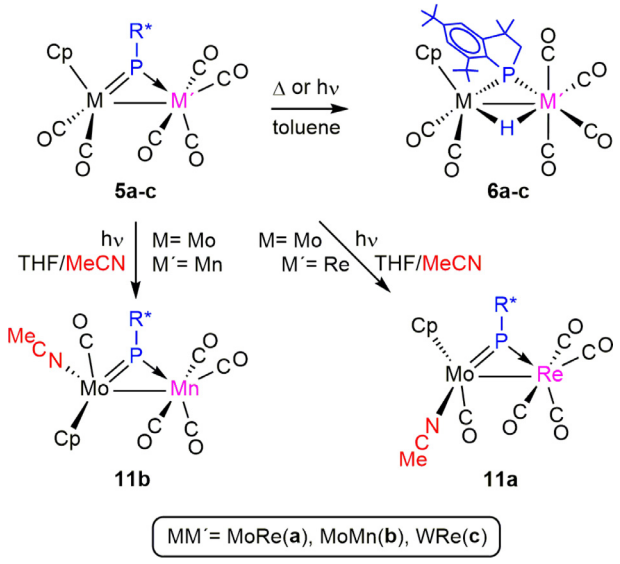

Scheme 6. Thermal and photochemical reactions of compounds **5**.

of heterometallic complexes **5a-d** in search for similar processes and possible heterometallic effects. As shown below, only the latter of the above processes was systematically observed for compounds **5**, while unexpected acetonitrile adducts were formed upon photolysis in tetrahydrofuran/acetonitrile mixtures, rather than products with metal-metal multiple bonds (Scheme 6).

As noted above, the MoRe complex **5a** rearranges upon irradiation with visible–UV light in toluene solution, to give the hydride-phosphanyl isomer [MoReCp(μ-H){μ-P(CH$_2$CMe$_2$)C$_6$H$_2$^{t}Bu$_2$}(CO)$_6$] (**6a**), as a result of the addition of a C–H bond of one ^{t}Bu group to the MoPRe center of the molecule. Such an isomerization can be also induced upon prolonged heating (ca. 7 h) in refluxing toluene solutions [2]. Surprisingly, its manganese analogue **5b** failed to rearrange upon visible-UV light irradiation in tetrahydrofuran or toluene solutions, even when using quartz glassware. In contrast, it undergoes rearrangement in refluxing toluene solution more easily than **5a** (completion in ca. 2 h) to give the corresponding hydride-phosphanyl isomer [MoMnCp(μ-H){μ-P(CH$_2$CMe$_2$)C$_6$H$_2$^{t}Bu$_2$}(CO)$_6$] (**6b**), although this reaction is less selective and gives substantial amounts of the mononuclear complex **1a**, thus evidencing significant breakdown of the binuclear structure along the process. Yet, the heterometallic effect on this C–H activation process seems clear. The tungsten complexes **5c,d** proved to be rather stable in refluxing toluene solutions, with no transformation being observed after a few hours. Upon prolonged irradiation (ca. 5 h) the WRe complex **5c** completed its rearrangement into the corresponding hydride isomer [WReCp(μ-H){μ-P(CH$_2$CMe$_2$)C$_6$H$_2$^{t}Bu$_2$}(CO)$_6$] (**6c**), whereas the manganese complex **5d** just underwent a generalized decomposition. In all, there seems to be a genuine heterometallic effect in this sort of transformations, which are generally easier for compounds **5** than for the dimolybdenum complex [Mo$_2$Cp$_2$(μ-PR*)(CO)$_4$], and are easier for combinations having lighter metals under thermal activation.

In our work on the Mo$_2$ complex mentioned above we found that the use of tetrahydrofuran/acetonitrile mixtures as solvent in the photochemical reactions fully suppressed the reaction pathway leading to its hydride isomer, then allowing for alternative reaction pathways to prevail [34b]. A similar effect was observed for our heterometallic complexes, although with different output. Indeed, irradiation of complexes **5a,b** with visible-UV light in tetrahydrofuran/acetonitrile (10/1) solutions yielded only mi-

nor amounts of the corresponding hydride isomers **6a,b**, and the major products now were the acetonitrile complexes [MoMCp(μ-PR*)(CO)$_5$(1κ-NCMe)] (M = Re (**11a**), Mn (**11b**), Scheme 6). These complexes could be isolated in moderate yield upon chromatographic workup and display different conformations, to be discussed below. We note the relatively unexpected regioselectivity of this carbonyl substitution reaction, as it involves the metal center (Mo) having a lower number of carbonyl ligands. Such a selectivity is likely due to the photochemical (rather than thermal) conditions used to induce decarbonylation in compounds **5**, and has been previously observed in the photochemical decarbonylation of the heterometallic phosphanyl-bridged complex [MoRe(μ-H)(μ-PCy$_2$)(CO)$_6$] in acetonitrile solution. The latter gives first complex [MoReCp(μ-H)(μ-PCy$_2$)(CO)$_5$(1κ-NCMe)], with an acetonitrile molecule bound to the Mo atom, which then progressively rearranges at room temperature to give the more stable isomer [MoReCp(μ-H)(μ-PCy$_2$)(CO)$_5$(2κ-NCMe)], with the acetonitrile ligand now bound to the Re atom [36].

2.6.1. Structure of hydride complexes 6

Spectroscopic data for compounds **6a-c** (Table 1 and Experimental section) are similar to each other, and dramatically different from those of their precursors. In the first place, they all show poorly deshielded ^{31}P NMR resonances in the range 40–150 ppm, some 520–590 ppm lower than the corresponding resonances in their parent precursors, which is indicative of the transformation of the phosphinidene ligand into a phosphanyl group. The ^{1}H NMR spectra reveal the presence of a bridging hydride ligand in each case (δ_H ca. −13 to −15 ppm), originated in one of the ^{t}Bu groups, now left with inequivalent CMe_2 and CH_2 protons. In all, the proposed structure for compounds **6** is comparable to those previously determined crystallographically for the related phosphanyl-bridged complexes [MM'Cp(μ-H)(μ-PPh$_2$)(CO)$_6$] (MM' = MoMn [37], [37a], MoRe [37b], WMn [37c]). A standard NOESY experiment on **6a** revealed the presence of positive NOE effects between the H atoms of the Cp ligand and those of the PCH_2 fragment, and presumably compounds **6b,c** would display the same conformation, which leaves the remaining *ortho*-^{t}Bu of the molecule far away from the Cp ligand, thus minimizing steric repulsions.

2.6.2. Structure of acetonitrile complexes 11

Spectroscopic data for compounds **11a,b**, to be discussed below, indicated significant differences between these seemingly similar complexes, so we decided to determine their structures crystallographically. As expected, the molecules of both complexes in the crystal (Fig. 6 and Table 6) are built from MoCp(CO)(NCMe) and M(CO)$_4$ fragments bridged by a phosphinidene ligand and further connected by an intermetallic bond. The latter bonds can be

Table 6
Selected bond lengths (Å) and angles (°) for compounds **11a** and **11b**.

	11a	11b
Mo1–*M*	3.1382(6)	2.9867(6)
Mo1–P1	2.262(2)	2.266(1)
M – P1	2.400(1)	2.239(1)
Mo1–C1	1.958(6)	1.952(4)
Mo1–N1	2.134(5)	2.127(3)
N1–C6	1.136(8)	1.132(5)
P1–C13	1.832(6)	1.850(3)
Mo1–P1–*M*	84.57(5)	83.06(3)
Mo1–P1–C13	126.4(2)	132.5(1)
M – P1–C13	148.7(2)	143.9(1)
P1–Mo1–C1	108.2(2)	79.8(1)
P1–Mo1–N1	105.4(1)	103.6(1)
C1–Mo1–N1	90.2(2)	91.5(1)
Mo–C1–O1	162.1(6)	175.7(3)

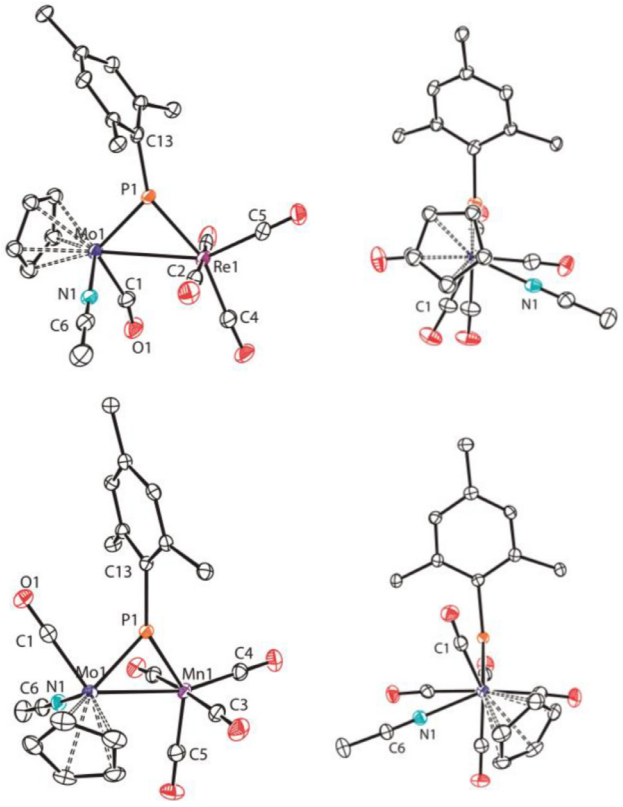

Fig. 6. ORTEP diagram (30% probability) of compounds **11a**, and **11b** with ^{t}Bu (except their C^1 atoms) and H atoms omitted for clarity. On the right, projections of the structures along the Mo–Re or Mo–Mn axis, respectively.

viewed as of similar length (3.1382(6) and 2.9867(6) Å), if we allow for the ca. 0.12 Å difference in the covalent radii of Re and Mn [23]. The Mo–P distances of ca. 2.26 Å in complexes **11** are comparable to the corresponding distance in the MoMn complex **5b**, and the P–Re/Mn bonds are a bit longer than the corresponding ones in complexes **5**. All of this justifies the classification of the electron distribution for the bridging phosphinidene ligand in these acetonitrile complexes in terms similar to those of their hexacarbonyl precursors (type **G** in Chart 1). Compounds **11a,b**, however, can be considered as rotational isomers, as they differ in the conformations of the MoCp(CO)(NCMe) fragment with respect to the MoPRe/Mn plane, which in turn are different from the conformation observed for the hexacarbonyl precursors **5a-c**. That conformation in the rhenium complex **11a** can be viewed as derived from a ca. 30° anticlockwise rotation of the Mo fragment in a conformation like the one observed in **5b** (Fig. 3), whereas a clockwise rotation of some 110° is needed to reach the observed conformation in **11b**. More importantly, this conformational difference has a significant impact on the Mo-bound carbonyl, which is pointing away from the dimetal center in **11b**, but is leaning toward the intermetallic region in **11a**, actually acquiring an incipient semibridging character (Mo1–C1–O1 = 162.1(6)°, Re···C(1) = 2.814(6) Å) [30].

The IR spectrum of **11a** in dichloromethane solution (Table 1) is consistent with its solid state structure, as it displays medium to strong bands in the range 2062–1923 cm^{-1} corresponding to a Re(CO)$_4$ oscillator with disphenoidal geometry, whereas the low-frequency band at 1751 cm^{-1} denotes the presence of a semibridging carbonyl. In contrast, the IR spectrum of **11b** in solution showed no low-frequency band, which is in agreement with the terminal nature of its Mo-bound carbonyl, as found in the crystal. The latter spectrum, however, displays a symmetrical stretch for

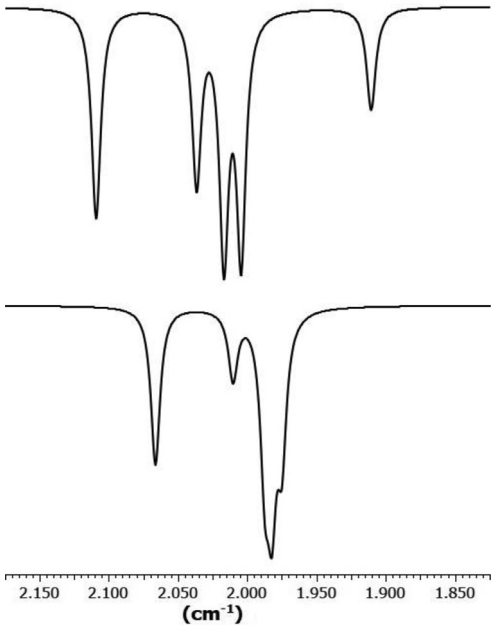

Fig. 7. M06L-DFT Computed IR spectra for compounds **11a** (upper) and **11b** (lower) in the C–O stretching region.

Table 7
M06L-DFT computed and experimental (dichloromethane solution) C – O stretching bands (cm^{-1}) for compounds **11**, along with their relative deviation (dev/%).

11a			**11b**		
Calcd.	Exp.	dev.	Calcd.	Exp.	dev.
2108	2062	+2.2	2066	2013	+2.6
2036	1968	+3.5	2010		
2016	1956	+3.1	1987	1926	+3.0
2003	1923	+4.2	1982		
1910	1751	+9.1	1974	1900	+3.9

its $Mn(CO)_4$ fragment of rather low energy (2013 cm^{-1}), and an extra weak band at 2034 cm^{-1}, perhaps indicative of the presence of a minor isomer in solution, not detected in the NMR spectra. To further support the retention in solution of the solid state structures of these compounds we performed density functional theory (DFT) calculations (see the Experimental section) [38], which yielded optimized structures in good agreement with the ones determined crystallographically (see the Supplementary material). The computed spectra in the C–O stretching region were also in good agreement with the experimental spectra in solution (Fig. 7 and Table 7), after allowing for some frequency overestimation expected in this sort of calculations (3–9% in our case) [39]. This indicates that the structures found for these compounds in the crystal are essentially retained in solution, and that the weak band at 2034 cm^{-1} appearing in the IR spectrum of the manganese complex **11b** most likely corresponds to a second, minor rotamer in fast equilibrium with the major isomer.

As noted above, the NMR spectra of compounds **11a,b** display resonances corresponding in each case to a single species in solution. We note the significant shielding by 100–150 ppm of the phosphinidene ^{31}P NMR resonance when going from compounds **5** to **11**, and the presence of single resonances corresponding to the Mo-bound acetonitrile ligand in the ^{1}H NMR spectra of the latter compounds, with chemical shifts (2.32 and 2.23 ppm) comparable to the one in the related phosphanyl-bridged complex [MoReCp(μ-H)(μ-PCy_2)$(CO)_5$(2κ-NCMe)] [35]. The transoid positioning of the semibridging carbonyl in **11a** with respect to the P atom (P1–Mo1–C1 = 108.2(2)°) is reflected in the absence of measurable P–C coupling in the corresponding ^{13}C NMR resonance [40]. Other spectroscopic data for compounds **11a,b** are as expected and deserve no further comments.

3. Conclusions

Three different synthetic approaches using the phosphanyl complexes *syn*-[MCp(PHR*)$(CO)_2$] (*M* = Mo, W; R* = 2,4,6-$C_6H_2{}^tBu_3$) as primary starting materials have been used to build heterometallic complexes connecting 15e $MCp(CO)_2$ fragments (*M* = Mo, W) with 17e M'$(CO)_n$ or MĆp$(CO)_n$ fragments (M = Mn, Re, Fe, Ru, Co) through a bridging PR* ligand. Photochemical reactions between the above phosphanyl complexes and dimers [M´$_2(CO)_{2n}$] or [M´$_2Cp_2(CO)_{2n}$] were generally of poor efficiency. Combinations with carbonyl-only containing metal fragments were best made through reaction between carbonylates [M'$(CO)_n]^-$ and chlorophosphanyl complexes [MCp(PClR*)$(CO)_2$], while combinations with Cp-containing metal fragments were best made by reacting Li[MoCp(PR*)$(CO)_2$] with the pertinent halide complexes [MXCp$(CO)_2$]. The primary products in these reactions were trigonal phosphinidene-bridged complexes of general formulae [MMĆp$_x$(μ-PR*)$(CO)_{n\ +\ 2}$] (x = 1, 2; *n* = 2, 4, 5), which were decarbonylated readily upon thermal or photochemical activation to yield the metal-metal bound derivatives [MMĆp$_x$(μ-PR*)$(CO)_{n\ +\ 1}$]. The latter contain two isoelectronic (15e) metal centers, whereby the trigonal phosphinidene ligand is expected to act as a 2e-donor to each of them. Yet, all structural data point to a description of the metal-phosphorus bonding in these complexes as a new asymmetric type of interaction (**G** in Chart 1), involving a M=P double bond to the group 6 metal, as found in mononuclear nucleophilic complexes, and a P→M' dative single bond to the other one, as found in mononuclear electrophilic complexes. Complexes [MMĆp(μ-PR*)$(CO)_6$] (M' = Mn, Re) undergo C–H bond cleavage in one ^{t}Bu group of the phosphinidene ligand upon thermal or photochemical activation, to eventually give the hydride-phosphanyl isomers [MMĆp(μ-H){μ-P(CH_2CMe_2)$C_6H_2{}^tBu_2$}$(CO)_6$]. This rearrangement takes place generally under milder conditions than those for the dimolybdenum complex [Mo_2Cp_2(μ-PR*)$(CO)_4$], and is also easier for combinations having lighter metals under thermal activation, thus pointing to a clear heterometallic effect. In the photochemical reactions of the Mo complexes, this process was suppressed by the presence of NCMe in the solvent, but then complexes [MoMĆp(μ-PR*)$(CO)_5$(1κ-NCMe)] were formed, with an acetonitrile molecule bound to the Mo atom and a coordination of the phosphinidene ligand similar to the one present in their parent compounds (type **G**).

4. Experimental

4.1. General procedures and starting materials

All manipulations and reactions were carried out under an argon (99.995%) atmosphere using standard Schlenk techniques. Solvents were purified according to literature procedures, and distilled prior to use [41]. Compounds [MoCp(PHR*)$(CO)_2$] (**1a**) and [MoCp(PClR*)$(CO)_2$] (**2a**) were prepared as described previously (Cp = η^5-C_5H_5; R* = 2,4,6-$C_6H_2{}^tBu_3$) [2,11]. Tetrahydrofuran solutions of Li[MoCp(PR*)$(CO)_2$] (**3**) were prepared in situ from **1a** as reported also by us [11]. Literature procedures were used in the preparation of complexes [$W_2Cp_2(CO)_6$] [42], [MCpX$(CO)_2$] (M = Fe, Ru; *X* = I, Br) [43], [AuCl{P(*p*-tol)$_3$}], (*p*-tol = 4-C_6H_4Me) [44], and for the preparation in situ of the anionic complexes Na[M$(CO)_5$] (M = Mn, Re) [45], and Na[Co$(CO)_4$] [46]. All other reagents were obtained from commercial suppliers and used as received, unless otherwise stated. Petroleum ether refers to that

fraction distilling in the range 338–343 K. Photochemical experiments were performed using jacketed Pyrex Schlenk tubes (unless otherwise stated) cooled by tap water (ca. 288 K) or by a closed 2-propanol circuit kept at the desired temperature with a cryostat. A 400 W medium-pressure mercury lamp placed ca. 1 cm away from the Schlenk tube was used for these experiments. Purging of liberated CO in these experiments was done by gently bubbling N_2 (99.9995%) through the solution. Filtrations were carried out through diatomaceous earth unless otherwise stated. Chromatographic separations were carried out using jacketed columns cooled as described above. Commercial aluminum oxide (activity I, 70–290 mesh) was degassed under vacuum prior to use. The latter was mixed under argon with the appropriate amount of water to reach activity IV. IR stretching frequencies of CO ligands were measured in solution (using CaF_2 windows), are referred to as ν(CO), and are given in wave numbers (cm^{-1}). Nuclear magnetic resonance (NMR) spectra were routinely recorded at 295 K unless otherwise stated. Chemical shifts (δ) are given in ppm, relative to internal tetramethylsilane (^1H, ^{13}C), or external 85% aqueous H_3PO_4 solutions (^{31}P). Coupling constants (J) are given in hertz.

4.2. Preparation of syn-[WCp(PHR*)(CO)$_2$] (1b)

A solution of $[W_2Cp_2(CO)_6]$ (0.400 g, 0.600 mmol) and PH_2R^* (0.167 g, 0.600 mmol) in tetrahydrofuran (10 mL) was irradiated with visible-UV light at 263 K for 1.5 h while gently bubbling N_2 (99.9995%), to give a dark purple solution. The solvent was then removed under vacuum, the residue was extracted with dichloromethane/petroleum ether (1/20), and the extracts were chromatographed on alumina at 258 K. Elution with the same solvent mixture gave a purple fraction yielding, after removal of solvents, compound **1b** as a purple solid (0.200 g, 57%). Anal. Calcd for $C_{25}H_{35}O_2PW$: C, 51.56; H, 6.06. Found: C, 51.25; H, 6.19. ν(CO) (petroleum ether): 1951 (vs), 1878 (s). ν(CO) (THF): 1939 (vs), 1860 (s). $^{31}P\{^1H\}$ NMR (121.48 MHz, C_6D_6): δ 213.3 (J_{PW} = 630). ^1H NMR (300.13 MHz, CD_2Cl_2): δ 12.61 (d, J_{HP} = 364, J_{HW} = 24, 1H, PH), 7.38 (d, J_{HH} = 2, 2H, C_6H_2), 5.46 (s, 5H, Cp), 1.48 (s, 18H, *o*-^{t}Bu), 1.33 (s, 9H, *p*-^{t}Bu). ^1H NMR (300.13 MHz, C_6D_6): δ 12.52 (d, J_{HP} = 367, 1H, PH), 7.42 (s, 2H, C_6H_2), 5.02 (s, 5H, Cp), 1.45 (s, 18H, *o*-^{t}Bu), 1.24 (s, 9H, *p*-^{t}Bu). $^{13}C\{^1H\}$ NMR (100.63 MHz, C_6D_6): δ 230.5 (d, J_{CP} = 12, WCO), 151.6 [s, $C^4(C_6H_2)$], 151.3 [s, $C^2(C_6H_2)$], 145.7 [d, J_{CP} = 14, $C^1(C_6H_2)$], 122.2 [d, J_{CP} = 7, $C^3(C_6H_2)$], 93.7 (s, Cp), 38.5 [s, C^1(*o*-^{t}Bu)], 35.0 [s, C^1(*p*-^{t}Bu)], 33.1 [s, C^2(*o*-^{t}Bu)], 31.3 [s, C^2(*p*-^{t}Bu)]. A standard NOESY experiment revealed the presence of positive NOE effects between the H atoms of the Cp ligand and those of the *o*-^{t}Bu groups.

4.3. Preparation of syn-[WCp(PClR*)(CO)$_2$] (2b)

Compound **1b** (0.040 g, 0.069 mmol) was dissolved in CCl_4 (1 mL) and the mixture was stirred at room temperature for 10 min to give a purple solution containing essentially pure compound **2b**. The solvent was then removed under vacuum to give a purple residue that can be used for further reactions without additional purification. Crystallization of the complex was achieved by the slow diffusion of a layer of petroleum ether into a concentrated toluene solution of the crude product at 253 K. This yielded dark purple crystals of compound **2b** (0.026 g, 61%). Anal. Calcd for $C_{25}H_{34}ClO_2PW$: C, 48.68; H, 5.56. Found: C, 48.35; H, 5.05. ν(CO) (petroleum ether): 1968 (vs), 1903 (s). $^{31}P\{^1H\}$ NMR (121.48 MHz, C_6D_6): δ 203.3 (br). ^1H NMR (300.13 MHz, C_6D_6): δ 7.51 (d, J_{HH} = 3, 2H, C_6H_2), 5.00 (s, 5H, Cp), 1.72 (s, 18H, *o*-^{t}Bu), 1.20 (s, 9H, *p*-^{t}Bu). $^{13}C\{^1H\}$ NMR (100.63 MHz, C_6D_6): δ 226.0 (d, J_{CP} = 16, WCO), 152.8 [s, $C^4(C_6H_2)$], 152.5 [s, br, $C^1(C_6H_2)$], 150.4 [s, $C^2(C_6H_2)$], 123.2 [d, J_{CP} = 6, $C^3(C_6H_2)$], 93.5 (s, Cp), 38.9 [s, C^1(*o*-^{t}Bu)], 35.3 [s, C^1(*p*-^{t}Bu)], 34.8 [s, C^2(*o*-^{t}Bu)], 31.2 [s, C^2(*p*-^{t}Bu)]. A standard NOESY experiment revealed the presence of positive NOE effects between the H atoms of the Cp ligand and those of the *o*-^{t}Bu groups.

4.4. Preparation of [MoMnCp(μ-PR*)(CO)$_7$] (4b)

Solid $Na[Mn(CO)_5]$ was prepared in situ by stirring an acetonitrile solution (6 mL) of $[Mn_2(CO)_{10}]$ (0.021 g, 0.054 mmol) with excess Na(Hg) (ca. 0.5 mL of a 0.5% amalgam, 1.5 mmol) for 20 min. This gave a gray suspension that was separated from the amalgam by transferring it into an empty Schlenk tube using a canula. The solvent was then removed under vacuum and the residue was washed with petroleum ether (3 × 3 mL) to give $Na[Mn(CO)_5]$ as a gray solid. Compound **2a**, prepared in situ from compound **1a** (0.049 g, 0.100 mmol) as described above, was then dissolved in dichloromethane (6 mL), the solution was cooled at 243 K and then transferred with a canula to the Schlenk tube containing the manganese complex. The mixture was stirred at 243 K for 15 min and then at room temperature for a further 10 min to give a brown solution. After removal of the solvent under vacuum, the residue was extracted with dichloromethane/petroleum ether (1/6), and the extracts were chromatographed on alumina at 258 K. Elution with the same solvent mixture gave first a purple fraction containing small amounts of compound **1a**, then a brown fraction yielding, after removal of solvents, compound **4b** as a brown microcrystalline solid (0.035 g, 51%). The crystals of **4b** used in the X-ray study were grown by the slow diffusion of a layer of petroleum ether into a concentrated dichloromethane solution of the complex at 253 K. Anal. Calcd for $C_{30}H_{34}MoMnO_7P$: C, 52.34; H, 4.98. Found: C, 52.05; H, 4.55. ^1H NMR (300.13 MHz, CD_2Cl_2): δ 7.34 (s, 2H, C_6H_2), 5.38 (s, 5H, Cp), 1.62 (s, 18H, *o*-^{t}Bu), 1.32 (s, 9H, *p*-^{t}Bu). $^{13}C\{^1H\}$ NMR (100.63 MHz, CD_2Cl_2, 253 K): δ 247.4 (d, J_{CP} = 14, MoCO), 207.5 (s, br, MnCO), 164.7 [d, J_{CP} = 49, $C^1(C_6H_2)$], 149.6 [s, $C^4(C_6H_2)$], 147.1 [s, $C^2(C_6H_2)$], 123.0 [s, $C^3(C_6H_2)$], 95.3 (s, Cp), 39.5 [s, C^1(*o*-^{t}Bu)], 35.1 [s, C^1(*p*-^{t}Bu)], 34.6 [s, C^2(*o*-^{t}Bu)], 31.2 [s, C^2(*p*-^{t}Bu)].

4.5. Preparation of [WReCp(μ-PR*)(CO)$_7$] (4c)

A solution of compounds **1b** (0.040 g, 0.069 mmol) and $[Re_2(CO)_{10}]$ (0.050 g, 0.077 mmol) in toluene (10 mL) was irradiated with visible-UV light at 288 K for 15 min while gently bubbling N_2 (99.9995%), to give a brown-greenish solution. The solvent was then removed under vacuum, the residue was extracted with dichloromethane/petroleum ether (1/12), and the extracts were chromatographed on silica gel at 258 K. Elution with dichloromethane/petroleum ether (1/20) gave first a brown fraction containing small amounts of compound **5c**, then a black fraction containing small amounts of the known $[W_2Cp_2(\mu\text{-}PR^*)(CO)_4]$ [10], and finally a green fraction. Removal of solvents under vacuum from the latter fraction yielded compound **4c** as a green solid (0.020 g, 32%). Anal. Calcd for $C_{30}H_{34}O_7PReW$: C, 39.70; H, 3.78. Found: C, 39.35; H, 3.25. ^1H NMR (300.13 MHz, CD_2Cl_2): δ 7.33 (s, 2H, C_6H_2), 5.33 (s, 5H, Cp), 1.60 (s, 18H, *o*-^{t}Bu), 1.34 (s, 9H, *p*-^{t}Bu). $^{13}C\{^1H\}$ NMR (100.63 MHz, CD_2Cl_2, 253 K): δ 241.4 (s, WCO), 182.0 (s, br, ReCO), 167.2 [d, J_{CP} = 43, $C^1(C_6H_2)$], 148.5 [s, $C^4(C_6H_2)$], 147.4 [s, $C^2(C_6H_2)$], 121.7 [s, $C^3(C_6H_2)$], 94.2 (s, Cp), 39.1 [s, C^1(*o*-^{t}Bu)], 35.1 [s, C^2(*o*-^{t}Bu)], 34.7 [s, C^1(*p*-^{t}Bu)], 30.9 [s, C^2(*p*-^{t}Bu)].

4.6. Preparation of [WMnCp(μ-PR*)(CO)$_7$] (4d)

The procedure is identical to the one described for compound **4b**, but now using $[Mn_2(CO)_{10}]$ (0.021 g, 0.054 mmol) and compound **1b** (0.058 g, 0.100 mmol) as starting products. This yielded a brown material containing **4d** as major species. Unfortunately, attempts to purify this crude product failed due to its

progressive transformation into **5d** upon manipulation, including low-temperature chromatography, so no elemental analysis was recorded for this material. ^{1}H NMR (300.13 MHz, CD_2Cl_2): δ 7.33 (s, 2H, C_6H_2), 5.43 (s, 5H, Cp), 1.63 (s, 18H, *o*-^{t}Bu), 1.32 (s, 9H, *p*-^{t}Bu).

4.7. Preparation of [MoMnCp(μ-PR*)(CO)$_6$] (5b)

A crude dichloromethane solution of compound **4b** was first obtained from compound **1a** (0.300 g, 0.607 mmol) and [$Mn_2(CO)_{10}$] (0.120 g, 0.308 mmol) as described above. After removal of the solvent under vacuum, the residue was dissolved in toluene (10 mL) and the solution was stirred at 338 K for 30 min to give a dark purple solution. The solvent was then removed, the residue extracted with dichloromethane/petroleum ether (1/20), and the extracts were chromatographed on silica gel at 258 K. Elution with the same solvent mixture gave first a yellow fraction containing small amounts of unidentified species, then a dark purple fraction. Removal of solvents from the latter fraction yielded compound **5b** as a dark purple microcrystalline solid (0.280 g, 70%). The crystals of **5b** used in the X-ray diffraction study were grown from a concentrated petroleum ether solution of the complex at 253 K. Anal. Calcd for $C_{30}H_{36}Cl_2MoMnO_6P$ (**5b**·CH_2Cl_2): C, 48.34; H, 4.87. Found: C, 48.13; H, 5.71. ν(CO) (Nujol): 2056 (s), 1975 (vs), 1940 (vs), 1926 (s), 1885 (m). ^{1}H NMR (300.13 MHz, CD_2Cl_2): δ 7.46 (s, 2H, C_6H_2), 5.16 (s, 5H, Cp), 1.48 (s, 18H, *o*-^{t}Bu), 1.39 (s, 9H, *p*-^{t}Bu). ^{13}C{^{1}H} NMR (100.63 MHz, CD_2Cl_2, 253 K): δ 230.0 (s, MoCO), 229.4 (s, br, MnCO), 223.7 (s, br, MnCO), 214.9 (d, J_{CP} = 22, 2MnCO), 152.1 [s, $C^4(C_6H_2)$], 151.6 [d, J_{CP} = 30, $C^1(C_6H_2)$], 150.5 [s, $C^2(C_6H_2)$], 122.2 [s, $C^3(C_6H_2)$], 93.1 (s, Cp), 38.4 [s, C^1(*o*-^{t}Bu)], 35.1 [s, C^1(*p*-^{t}Bu)], 32.6 [s, C^2(*o*-^{t}Bu)], 30.8 [s, C^2(*p*-^{t}Bu)].

4.8. Preparation of [WReCp(μ-PR*)(CO)$_6$] (5c)

A crude toluene solution of compound **4c**, obtained as described above, was stirred at 363 K for 20 min to give a brown solution. The solvent was then removed under vacuum, the residue was extracted with dichloromethane/petroleum ether (1/20), and the extracts were chromatographed on alumina at 258 K. Elution with the same solvent mixture gave first a brown fraction yielding, after removal of solvents, compound **5c** as a brown microcrystalline solid (0.036 g, 60%), then a black fraction containing small amounts of the known [W_2Cp_2(μ-PR*)(CO)$_4$] [10]. Elution with dichloromethane/petroleum ether (1/5) gave a green fraction yielding analogously small amounts of unreacted **4c**. Anal. Calcd for $C_{29}H_{34}O_6PReW$: C, 39.60; H, 3.90. Found: C, 39.32; H, 3.53. ^{1}H NMR (300.13 MHz, CD_2Cl_2): δ 7.43 (s, 2H, C_6H_2), 5.12 (s, 5H, Cp), 1.44 (s, 18H, *o*-^{t}Bu), 1.38 (s, 9H, *p*-^{t}Bu). ^{13}C{^{1}H} NMR (100.63 MHz, CD_2Cl_2): δ 219.4 (s, J_{CW} = 170, WCO), 198.7 (d, J_{CP} = 36, ReCO), 192.4 (s, ReCO), 187.2 (d, J_{CP} = 10, 2ReCO), 152.0 [s, $C^4(C_6H_2)$], 150.7 [s, $C^2(C_6H_2)$], 149.8 [d, J_{CP} = 21, $C^1(C_6H_2)$], 122.4 [d, J_{CP} = 8, $C^3(C_6H_2)$], 92.2 (s, Cp), 39.0 [s, C^1(*o*-^{t}Bu)], 35.4 [s, C^1(*p*-^{t}Bu)], 33.1 [s, C^2(*o*-^{t}Bu)], 31.2 [s, C^2(*p*-^{t}Bu)].

4.9. Preparation of [WMnCp(μ-PR*)(CO)$_6$] (5d)

A crude dichloromethane solution of compound **4d** was first obtained as described above by starting from **1b** (0.058 g, 0.100 mmol) and [$Mn_2(CO)_{10}$] (0.021 g, 0.054 mmol). After removal of the solvent, the residue was extracted with dichloromethane/petroleum ether and the extracts were chromatographed on alumina at 258 K to remove some **1b** formed in the reaction. Elution with the same solvent mixture gave first a yellow fraction containing small amounts of unidentified species, then a minor purple fraction containing **1b** and finally a brown fraction containing a mixture of compounds **4d** and **5d**. The latter fraction was stirred at room temperature for 3 h to give a solution of compound **5d**. The solvent was again removed, the residue was extracted with dichloromethane/petroleum ether (1/8), and the extracts were chromatographed on alumina at 258 K. Elution with the same solvent mixture gave a brown fraction yielding, after removal of solvents, compound **5d** as a dark purple microcrystalline solid (0.025 g, 39%). Anal. Calcd for $C_{29}H_{34}O_6MnPW$: C, 46.55; H, 4.58. Found: C, 46.39; H, 4.22. ^{1}H NMR (400.13 MHz, CD_2Cl_2): δ 7.42 (s, 2H, C_6H_2), 5.10 (s, 5H, Cp), 1.49 (s, 18H, *o*-^{t}Bu), 1.38 (s, 9H, *p*-^{t}Bu). ^{13}C{^{1}H} NMR (100.63 MHz, CD_2Cl_2): δ 218.8 (s, J_{CW} = 175, WCO), 152.9 [d, J_{CP} = 24, $C^1(C_6H_2)$], 152.3 [s, $C^4(C_6H_2)$], 150.5 [s, $C^2(C_6H_2)$], 122.2 [d, J_{CP} = 7, $C^3(C_6H_2)$], 91.8 (s, Cp), 38.7 [s, C^1(*o*-^{t}Bu)], 35.4 [s, C^1(*p*-^{t}Bu)], 33.0 [s, C^2(*o*-^{t}Bu)], 31.2 [s, C^2(*p*-^{t}Bu)]. No resonances could be identified in this spectrum as due to the Mn-bound carbonyls (they being presumably very broad).

4.10. Preparation of [MoMnCp(μ-H){μ-P(CH_2CMe_2)$C_6H_2{}^tBu_2$}(CO)$_6$] (6b)

A toluene solution (8 mL) of compound **5b** (0.040 g, 0.061 mmol) was refluxed for 2 h to give a greenish solution containing a ca. 1:1 mixture of compounds **1a** and **6b**. After removal of the solvent under vacuum, the residue was extracted with petroleum ether, and the extracts were chromatographed on alumina at 258 K. Elution with the same solvent gave a purple fraction containing the phosphanyl complex **1a**. Elution with dichloromethane/petroleum ether (1/20) gave a yellow fraction yielding, after removal of solvents, compound **6b** as a yellow microcrystalline solid (0.012 g, 30%). Anal. Calcd for $C_{29}H_{34}MoMnO_6P$: C, 52.74; H, 5.19. Found: C, 52.25; H, 4.89. ^{1}H NMR (400.13 MHz, CD_2Cl_2): δ 7.40 (d, J_{HP} = 5, J_{HH} = 2, 1H, C_6H_2), 7.26 (s, 1H, C_6H_2), 5.24 (s, 5H, Cp), 3.40 (t, $J_{HH} \sim J_{HP}$ = 14, 1H, PCH_2), 2.10 (dd, J_{HH} = 13, J_{HP} = 8, 1H, PCH_2), 1.50, 1.49 (2 s, 2 × 3H, CMe_2), 1.36, 1.21 (2 s, 2 × 9H, ^{t}Bu), −13.30 (d, J_{HP} = 33, 1H, μ-H). ^{13}C{^{1}H} NMR (100.63 MHz, CD_2Cl_2): δ 241.5 (d, J_{CP} = 25, MoCO), 235.5 (s, MoCO), 218.9 (s, br, 2MnCO), 211.6, 210.0 (2 s, br, MnCO), 158.6 [d, J_{CP} = 14, $C^{2,6}(C_6H_2)$], 154.4 [d, J_{CP} = 7, $C^{6,2}(C_6H_2)$], 153.6 [s, $C^4(C_6H_2)$], 135.4 [d, J_{CP} = 19, $C^1(C_6H_2)$], 123.2 [d, J_{CP} = 9, $C^{3,5}(C_6H_2)$], 119.1 [d, J_{CP} = 9, $C^{5,3}(C_6H_2)$], 92.4 (s, Cp), 56.5 (d, J_{CP} = 23, PCH_2), 44.6 (s, CMe_2), 38.2 (s, Me), 35.3 [s, C^1(^{t}Bu)], 32.6 [s, C^2(^{t}Bu)], 31.9 [d, J_{CP} = 8, C^1(^{t}Bu)], 31.3 [s, C^2(^{t}Bu)], 29.7 (s, Me).

4.11. Preparation of [WReCp(μ-H){μ-P(CH_2CMe_2)$C_6H_2{}^tBu_2$}(CO)$_6$] (6c)

A toluene solution (8 mL) of compound **5c** (0.025 g, 0.028 mmol) was irradiated with visible-UV light at 288 K for 5 h to give an orange solution. The solvent was then removed under vacuum, the residue was extracted with dichloromethane/petroleum ether (1/20), and the extracts were chromatographed on alumina at 258 K. Elution with the same solvent mixture gave first a minor brown fraction containing unreacted **5c**, then a major yellow fraction yielding, after removal of solvents, compound **6c** as a yellow microcrystalline solid (0.015 g, 60%). Anal. Calcd for $C_{29}H_{34}O_6PWRe$: C, 39.60; H, 3.90. Found: C, 39.25; H, 3.54. ^{1}H NMR (400.13 MHz, CD_2Cl_2): δ 7.37 (dd, J_{HP} = 5, J_{HH} = 2, 1H, C_6H_2), 7.23 (d, J_{HH} = 2, 1H, C_6H_2), 5.35 (s, 5H, Cp), 3.36 (t, J_{HH} = J_{HP} = 13, 1H, PCH_2), 1.97 (dd, J_{HH} = 13, J_{HP} = 6, 1H, PCH_2), 1.49, 1.45 (2 s, 2 × 3H, CMe_2), 1.35, 1.28 (2 s, 2 × 9H, ^{t}Bu), −14.78 (d, J_{HP} = 15, J_{HW} = 50, 1H, μ-H). ^{13}C{^{1}H} NMR (100.63 MHz, CD_2Cl_2): δ 230.6 (d, J_{CP} = 17, WCO), 224.9 (s, WCO), 186.8 (d, J_{CP} = 32, ReCO), 184.6 (s, br, ReCO), 183.6 (d, J_{CP} = 6, ReCO), 183.5 (d, J_{CP} = 7, ReCO), 158.3 [d, J_{CP} = 16, $C^{2,6}(C_6H_2)$], 154.4 [d, J_{CP} = 6, $C^{6,2}(C_6H_2)$], 153.1 [s, $C^4(C_6H_2)$], 132.5 [d, J_{CP} = 29, $C^1(C_6H_2)$], 123.2 [d, J_{CP} = 9, $C^{3,5}(C_6H_2)$], 119.0 [d, J_{CP} = 10, $C^{5,3}(C_6H_2)$], 90.4 (s, Cp), 56.1 (d, J_{CP} = 29, PCH_2), 45.6

(s, CMe_2), 38.4 (s, Me), 35.3 [s, $C^1(^t$Bu)], 32.7 [s, $C^2(^t$Bu)], 32.2 [d, J_{CP} = 9, $C^1(^t$Bu)], 31.3 [s, $C^2(^t$Bu)], 29.7 (s, Me).

4.12. New preparation of [MoCoCp(μ-PR*)(CO)$_5$] (7)

A colorless solution of Na[Co(CO)$_4$] was prepared in situ by stirring [Co$_2$(CO)$_8$] (0.024 g, 0.070 mmol) and excess NaOH (ca. 0.020 g, 0.5 mmol) in tetrahydrofuran (8 mL) for 10 min. Using a canula, the solution was transferred into a Schlenk tube containing solid compound **2a**, prepared in situ from compound **1a** (0.050 g, 0.101 mmol) as described previously. Solvent was then removed under vacuum and the mixture was dissolved in dichloromethane (8 mL) to give instantaneously a green solution. After removal of the solvent under vacuum, the residue was extracted with dichloromethane/petroleum ether (1/20), and the extracts were chromatographed on alumina at 258 K. Elution with the same solvent mixture gave a green fraction yielding, after removal of solvents, compound **7** as a green microcrystalline solid (0.050 g, 78%). Spectroscopic data for this product were identical to those previously described for compound **7** [7].

4.13. Preparation of [MoRuCp$_2$(μ-PR*)(CO)$_4$] (8f)

^{n}BuLi (50 μL of a 1.6 M solution in hexane, 0.080 mmol) was added to a tetrahydrofuran solution (8 mL) of compound **1a** (0.030 g, 0.061 mmol) at 195 K, and the mixture was stirred for 1 min to give a dark green solution of Li[MoCp(PR*)(CO)$_2$] (**3**). This solution was then transferred using a canula into a Schlenk tube equipped with a teflon Youngś valve containing solid [RuBrCp(CO)$_2$] (0.018 g, 0.059 mmol), and the mixture was stirred at room temperature for 7 days, to give a brown solution containing compound **8f** as the major product. The solvent was then removed under vacuum, the residue was extracted with dichloromethane/petroleum ether (1/4), and the extracts were chromatographed on alumina at 258 K. Elution with the same solvent mixture gave a minor purple fraction containing small amounts of **1a**, then a yellow fraction containing small amounts of uncharacterized species, and finally a major green fraction yielding, after removal of solvents, compound **8f** as a green solid (0.020 g, 47%). Anal. Calcd for $C_{32}H_{39}MoO_4PRu$: C, 53.71; H, 5.49. Found: C, 53.35; H, 5.25. ^{1}H NMR (300.13 MHz, CD_2Cl_2): δ 7.37 (s, 2H, C_6H_2), 5.47, 5.10 (2 s, 2 × 5H, Cp), 1.60 (s, 18H, *o*-^{t}Bu), 1.34 (s, 9H, *p*-^{t}Bu). $^{13}C\{^1H\}$ NMR (100.63 MHz, CD_2Cl_2): δ 249.0 (d, J_{CP} = 15, MoCO), 199.0 (d, J_{CP} = 12, RuCO), 164.6 [d, J_{CP} = 45, $C^1(C_6H_2)$], 148.9 [s, $C^4(C_6H_2)$], 148.0 [s, $C^2(C_6H_2)$], 123.1 [d, J_{CP} = 4, $C^3(C_6H_2)$], 94.5 (s, MoCp), 90.9 (s, RuCp), 40.0 [s, C^1(*o*-^{t}Bu)], 35.9 [s, C^2(*o*-^{t}Bu)], 35.2 [s, C^1(*p*-^{t}Bu)], 31.1 [s, C^2(*p*-^{t}Bu)].

4.14. VT NMR data for [MoFeCp$_2$(μ-PR*)(CO)$_3$] (9e)

$^{31}P\{^1H\}$ NMR (162.23 MHz, CD_2Cl_2, 223 K): δ 662.6 (br). $^{31}P\{^1H\}$ NMR (162.23 MHz, CD_2Cl_2, 193 K): δ 675.1 (br, isomer *trans*), 628.5 (br, isomer *cis*); ratio *trans*/*cis* ca. 3/1. ^{1}H NMR (300.13 MHz, CD_2Cl_2): δ 7.48 (s, 2H, C_6H_2), 5.23, 4.51 (2 s, 2 × 5H, Cp), 1.64, 1.47 (2 s, br, 2 × 9H, *o*-^{t}Bu), 1.38 (s, 9H, *p*-^{t}Bu). ^{1}H NMR (400.54 MHz, CD_2Cl_2, 193 K): δ 7.50 (s, 2H, C_6H_2), 5.35 (s, 5H, MoCp), 4.58 (s, br, 5H, FeCp), 1.68, 1.45, 1.38 (3 s, br, 3 × 9H, ^{t}Bu). $^{13}C\{^1H\}$ NMR (100.63 MHz, CD_2Cl_2): δ 258.0, 254.2 (2s, MoCO), 219.9 (d, J_{CP} = 16, FeCO), 153.6, 152.6 [2 s, br, $C^2(C_6H_2)$], 152.8 [s, $C^4(C_6H_2)$], 151.0 [d, J_{CP} = 45, $C^1(C_6H_2)$], 123.6, 123.3 [2 s, br, $C^3(C_6H_2)$], 94.4 (s, MoCp), 85.4 (s, FeCp), 39.2 [s, 2C^1(*o*-^{t}Bu)], 35.7 [s, C^1(*p*-^{t}Bu)], 33.9, 32.9 [2 s, br, C^2(*o*-^{t}Bu)], 31.3 [s, C^2(*p*-^{t}Bu)]. $^{13}C\{^1H\}$ NMR (100.73 MHz, CD_2Cl_2, 193 K): δ 219.9 (s, br, FeCO), 153.3, 153.0 [2 s, br, $C^2(C_6H_2)$], 152.3 [s, $C^4(C_6H_2)$], 149.5 [d, J_{CP} = 45, $C^1(C_6H_2)$], 123.7, 123.2 [2 s, br, $C^3(C_6H_2)$], 94.9 (s, MoCp), 85.4 (s, FeCp), 38.9 [s, 2C^1(*o*-^{t}Bu)], 35.5 [s, C^1(*p*-^{t}Bu)], 33.3, 32.4 [2 s, br, C^2(*o*-^{t}Bu)], 30.9 [s, C^2(*p*-^{t}Bu)]. Resonances for the Mo-bound carbonyls could not be identified in the spectrum at this temperature.

4.15. Preparation of [MoRuCp$_2$(μ-PR*)(CO)$_3$] (9f)

A tetrahydrofuran solution (6 mL) of compound **8f** (0.030 g, 0.042 mmol) was irradiated with visible-UV light at 288 K for 20 min while keeping a gentle N_2 (99.9995%) purge, to get a brown solution. The solvent was then removed under vacuum, the residue was extracted with dichloromethane/petroleum ether (1/8), and the extracts were chromatographed on silica gel at 258 K. Elution with dichloromethane/petroleum ether (1/3) gave minor orange and yellow fractions containing unidentified species. Elution with dichloromethane/petroleum ether (3/1) gave a major brown fraction yielding, after removal of solvents, compound **9f** as a brown solid (0.015 g, 52%). Anal. Calcd for $C_{31}H_{39}MoO_3PRu$: C, 54.15; H, 5.72. Found: C, 53.80; H, 5.35. ^{1}H NMR (300.13 MHz, CD_2Cl_2): δ 7.46 (s, 2H, C_6H_2), 5.26, 5.10 (2 s, 2 × 5H, Cp), 1.55 (s, br, 18H, *o*-^{t}Bu), 1.36 (s, 9H, *p*-^{t}Bu). $^{13}C\{^1H\}$ NMR (100.63 MHz, CD_2Cl_2): δ 255.9 (s, MoCO), 253.3 (d, J_{CP} = 14, MoCO), 208.9 (d, J_{CP} = 9, RuCO), 153.0 [s, $C^2(C_6H_2)$], 152.7 [s, $C^4(C_6H_2)$], 148.8 [d, J_{CP} = 41, $C^1(C_6H_2)$], 123.3 [d, J_{CP} = 6, $C^3(C_6H_2)$], 94.2 (s, MoCp), 89.2 (s, RuCp), 39.2 [s, C^1(*o*-^{t}Bu)], 35.6 [s, C^1(*p*-^{t}Bu)], 33.5 [s, br, C^2(*o*-^{t}Bu)], 31.2 [s, C^2(*p*-^{t}Bu)].

4.16. New preparation of [MoAuCp(μ-PR*)(CO)$_2${P(p-tol)$_3$}] (10)

The method is similar to the one described above for **8f**, but starting from 0.020 g (0.040 mmol) of **1a**, and using [AuCl{P(*p*-tol)$_3$}] (0.022 g, 0.040 mmol) instead of the ruthenium complex. This yielded a greenish solution. After removal of the solvent, the residue was extracted with dichloromethane, and the extracts were filtered to give a green solution which was concentrated under vacuum. X-ray quality crystals of **10** were grown by the slow diffusion of a layer of petroleum ether into a concentrated dichloromethane solution of the complex (0.024 g, 60%). Spectroscopic data for this product were identical to those previously described for compound **10** [11].

4.17. Preparation of [MoReCp(μ-PR*)(CO)$_5$(1k-NCMe)] (11a)

A THF/MeCN solution (8 mL of a 10:1 mixture) of compound **5a** (0.030 g, 0.038 mmol) was irradiated with visible-UV light at 263 K for 2 h while gently bubbling N_2 (99.9995%), to give a yellow solution containing **11a** as major product, along with some **6a** and other phosphanyl-containing species, not investigated. The solvent was then removed under vacuum, the residue was extracted with dichloromethane/petroleum ether (1/8), and the extracts were chromatographed on alumina at 258 K. Elution with the same solvent mixture gave first a minor brown fraction containing a small amount of unreacted **5a**, then a yellow fraction yielding, after removal of solvents, compound **11a** as an air-sensitive yellow microcrystalline solid (0.015 g, 50%). The crystals of **11a** used in the X-ray diffraction study were grown through the slow solution of a layer of petroleum ether into a concentrated dichloromethane solution of the complex at 253 K. Anal. Calcd for $C_{30}H_{37}NMoO_5PRe$: C, 44.77; H, 4.63; N, 1.74. Found: C, 44.45; H, 4.25; N, 1.50. ^{1}H NMR (400.13 MHz, CD_2Cl_2): δ 7.49, 7.39 (2s, 2 × 1H, C_6H_2), 4.90 (s, 5H, Cp), 2.32 (s, 3H, NCMe), 1.44, 1.43, 1.37 (3 s, 3 × 9H, ^{t}Bu). $^{13}C\{^1H\}$ NMR (100.63 MHz, CD_2Cl_2): δ 240.0 (s, MoCO), 200.2 (d, J_{CP} = 36, ReCO), 193.6 (s, ReCO), 189.9 (d, J_{CP} = 9, ReCO), 188.6 (d, J_{CP} = 11, ReCO), 155.4, 151.0 [2 s, $C^{2,6}(C_6H_2)$], 149.8 [s, $C^4(C_6H_2)$], 147.7 [d, J_{CP} = 28, $C^1(C_6H_2)$], 146.4 [s, br, NCMe], 122.9 [d, J_{CP} = 7, $C^{3,5}(C_6H_2)$], 121.9 [d, J_{CP} = 5, $C^{5,3}(C_6H_2)$], 94.4 (s, Cp), 39.3, 38.9, 35.4 [3 s, $C^1(^t$Bu)], 33.3, 32.5 [2 s, br, C^2(*o*-^{t}Bu)], 31.3 [s, C^2(*p*-^{t}Bu)], 5.4 (s, NC*Me*).

4.18. Preparation of [MoMnCp(μ-PR*)(CO)$_5$(1k-NCMe)] (11b)

A THF/MeCN solution (6 mL of a 10:1 mixture) of compound **5b** (0.020 g, 0.030 mmol) was irradiated in a quartz jacketed Schlenk tube with visible-UV light at 263 K for 7 h with a gentle N_2 (99.9995%) purge, to give a brown solution. The solvent was then removed under vacuum, the residue was extracted with dichloromethane/petroleum ether (1/6), and the extracts were chromatographed on alumina at 258 K. Elution with the same solvent mixture gave first a minor purple fraction containing a small amount of unreacted **5b**, then minor pink and blue fractions containing unidentified species. Elution with dichloromethane/petroleum ether (1/2) gave an orange fraction yielding, after removal of solvents, compound **11b** as an orange microcrystalline solid (0.008 g, 20%). The crystals of **11b** used in the X-ray diffraction study were grown through the slow diffusion of a layer of petroleum ether into a concentrated dichloromethane solution of the complex at 253 K. Anal. Calcd for $C_{30}H_{37}NMoMnO_5P$: C, 53.50; H, 5.54; N, 2.08. Found: C, 53.05; H, 5.15; N, 1.80. ^{1}H NMR (400.13 MHz, CD_2Cl_2): δ 7.44, 7.41 (2s, 2 $\times$ 1H, C_6H_2), 5.15 (s, br, 5H, Cp), 2.24 (s, 3H, NCMe), 1.62 (s, br, 9H, ^{t}Bu), 1.36 (s, 9H, ^{t}Bu), 1.17 (s, br, 9H, ^{t}Bu).

4.19. X-Ray structure determination of compounds 4b, 9f, 10, 11a and 11b

Data collection for these compounds was performed at ca. 155 K on an Oxford Diffraction Xcalibur Nova single crystal diffractometer, using Cu Kα radiation. Images were collected at a 62 mm fixed crystal-detector distance using the oscillation method, with 1.0–1.3° oscillation and variable exposure time per image. Data collection strategy was calculated with the program *CrysAlis Pro-CCD* [47], and data reduction and cell refinements were performed with the program *CrysAlis Pro-RED* [47]. In both cases, an empirical absorption correction was applied using the SCALE3 ABSPACK algorithm as implemented in the program *CrysAlis Pro-RED*. Using the program suite WinGX [48], the structures were solved by Patterson interpretation and phase expansion using SHELXL2018/3 [49], and refined with full-matrix least squares on F^2 using SHELXL2018/3. In general, all non-hydrogen atoms were refined anisotropically, except for atoms involved in disorder, and all hydrogen atoms were geometrically placed and refined using a riding model. In compound **9f** two similar but independent molecules were present in the unit cell; one of them displayed disordered cyclopentadienyl ligands, each of them satisfactorily modeled over two positions with 0.50/0.50 occupancies. In compound **10**, one ^{t}Bu group and the Cp ligand were disordered and satisfactorily modeled over two positions with 0.70/0.30 occupancies. The disordered carbon atoms were refined isotropically, and this caused a B-level alert in the corresponding checkcif file. In compound **11a**, the Cp ligand was disordered, and satisfactorily modeled over two positions with 0.65/0.45 occupancies. The disordered carbon atoms were refined isotropically, and this also caused a B-level alert in the corresponding checkcif file. Compound **11b** crystallized with a molecule of dichloromethane, satisfactorily refined. Other data for the refinements of these structures can be found in the Supplementary Material (Tables S1 and S2).

4.20. X-Ray structure determination of compound 5b

Data collection for this compound was performed at 100 K on a Bruker D8 Venture Photon III 14 κ-geometry diffractometer, using MoK$_\alpha$ radiation. The software APEX3 [50] was used for collecting frames with the ω/ϕ scan measurement method. The SAINT V8.40B software was used for data reduction [51], and a multiscan absorption correction was applied with SADABS-2016/2 [52]. The solution of the structure and refinements was performed as described above to give the residuals shown in Table S1.

4.21. Computational details

All DFT calculations were carried out using the GAUSSIAN16 package [53], and the M06L functional [54]. A pruned numerical integration grid (99,590) was used for all the calculations via the keyword Int=Ultrafine together with the empirical dispersion correction from Grimme and co-workers via the keyword GD3 [55]. Effective core potentials and their associated double-ζ LANL2DZ basis set were used for Mo, Re and Mn atoms [56]. The light elements (P, C, N, O and H) were described with the cc-pVDZ basis sets of Dunning and coworkers [57]. Geometry optimizations were performed under no symmetry restrictions, using initial coordinates derived from the X-ray data. Frequency analysis was performed for all the stationary points to ensure that a minimum structure with no imaginary frequencies was achieved in each case.

Declaration of Competing Interest

The authors declare that they have no known competing financial interests or personal relationships that could have appeared to influence the work reported in this paper.

Data Availability

Data will be made available on request.

Acknowledgements

We thank the MICIU and AEI of Spain and FEDER for financial support (Project PGC2018–097366-B-I00), the SCBI of the Universidad de Málaga, Spain, for access to computing facilities, and the X-Ray units of the Universidad de Oviedo and Universidad de Santiago de Compostela, Spain, for acquisition of diffraction data.

Supplementary materials

Supplementary material associated with this article can be found, in the online version, at doi:10.1016/j.jorganchem.2022.122460.

References

[1] [a] M.E. García, D. García-Vivó, A. Ramos, M.A. Ruiz, Coord. Chem. Rev. 330 (2017) 1; [b] G. Huttner, K. Evertz, Acc. Chem. Res. 19 (1986) 406; [c] G. Huttner, K. Knoll, Angew. Chem. Int. Ed. Engl. 26 (1987) 743.
[2] M.A. Alvarez, M.E. García, D. García-Vivó, M.A. Ruiz, P. Vega, Inorg. Chem. 59 (2020) 9481.
[3] For some recent reviews see
[a] F. Mathey, Z. Duan, Dalton Trans. 45 (2016) 1804.
[b] H. Aktas, J.C. Slootweg, K. Lammertsma, Angew. Chem. Int. Ed. 49 (2010) 2102.
[c] R. Waterman, Dalton Trans. (2009) 18.
[d] F. Mathey, Dalton Trans. (2007) 1861.
[4] [a] M. Knorr, I. Jourdain, Coord. Chem. Rev. 350 (2017) 217; [b] N.P. Mankad, Chem. Eur. J. 22 (2016) 5822; [c] P. Buchwalter, J. Rosé, P. Braunstein, Chem. Rev. 115 (2015) 28.
[5] U.A. Hirth, W. Malisch, J. Organomet. Chem. 439 (1992) C16.
[6] H. Lang, M. Winter, M. Leise, O. Walter, L. Zsolnai, J. Chem. Soc., Chem. Commun. (1994) 595.
[7] [a] B. Alvarez, M.A. Alvarez, I. Amor, M.E. García, M.A. Ruiz, Inorg. Chem. 50 (2011) 10561; [b] B. Alvarez, M.A. Alvarez, M.E. García, M.A. Ruiz, Dalton Trans 45 (2016) 1937.
[8] B. Alvarez, M.A. Alvarez, I. Amor, M.E. García, D. García-Vivó, M.A. Ruiz, Inorg. Chem. 57 (2018) 1901.
[9] J. Sánchez-Nieves, B.T. Sterenberg, K.A. Udachin, A.J. Carty, Inorg. Chim. Acta 350 (2003) 486.
[10] R. Schmitt, Ph. D. Thesis, Julius Maximiliams University of Würzburg, 2005.
[11] M.A. Alvarez, M.E. García, D. García-Vivó, M.A. Ruiz, P. Vega, Dalton Trans 48 (2019) 14585.
[12] M.A. Angeles, M.E. García, V. Riera, M.A. Ruiz, C. Bois, Y. Jeannin, J. Am. Chem. Soc. 117 (1995) 1324.

[13] R.B. King, Organometallic Synthesis Vol. I (Transition Metal Compounds), Academic Press, Oxford, U. K, 1965 chapter H.
[14] W. Malisch, U. Hirth, K. Grün, M. Schmeusser, J. Organomet. Chem. 572 (1999) 207.
[15] The thermal routes reported by Malisch et al. for the tungsten complex (ref. 14) might have yielded small amounts of the *syn* isomer **1b**, since Schmitt actually determined the structure of a crystal of this isomer grown from the product formed by following these thermal methods. The measured W−P length in **1b** was very short (2.247(1) Å), as expected for a double bond. Unfortunately, no spectroscopic data were given at the time for this crystalline material (see ref. 10), so comparisons with our current data are not possible.
[16] M. Alonso, M.A. Alvarez, M.E. García, D. García-Vivó, M.A. Ruiz, Inorg. Chem. 49 (2010) 8962.
[17] A.H. Cowley, D.M. Giolando, C.M. Nunn, M. Pakulski, D. Westmoreland, N.C. Norman, J. Chem. Soc., Dalton Trans. (1988) 2127.
[18] P.S. Braterman, Metal Carbonyl Spectra, Academic Press, London, U. K., 1975.
[19] C.J. Jameson, in Phosphorus-31 NMR Spectroscopy in Stereochemical Analysis, J.G.Verkade, L.D. Quin, Eds., VCH, Deerfield Beach, FL, 1987, Chapter 6.
[20] M.A. Alvarez, M.E. García, D. García-Vivó, M.A. Ruiz, A. Toyos, Inorg. Chem. 57 (2018) 2228.
[21] A.M. Arif, A.H. Cowley, N.C. Norman, A.G. Orpen, M. Pakulski, Organometallics 7 (1988) 309.
[22] K. Jörg, W. Malisch, W. Reich, A. Meyer, U. Schubert, Angew. Chem. Int. Ed. Engl. 25 (1986) 92.
[23] B. Cordero, V. Gómez, A.E. Platero-Prats, M. Revés, J. Echevarría, E. Cremades, F. Barragán, S. Alvarez, Dalton Trans. 2008, 2832.
[24] E. Lindner, M. Darmuth, H.A. Mayer, R. Fawzi, C. Maichle, M. Steimann, Chem. Ber. 126 (1993) 23.
[25] A.J. Carty, S.A. MacLaughlin, D. Nucciarone, in Phosphorus-31 NMR Spectroscopy in Stereochemical Analysis, J.G. Verkade, L.D. Quin, Eds., VCH, Deerfield Beach, FL, 1987, Chapter 16.
[26] For the X-ray determined structure of [WReCp(μ-PR*)(CO)6] (**5c**) see: M.A. Alvarez, M.E. García, M.A. Ruiz, P. Vega, CSD Communication, 2019. CCDC 1908769, doi: 10.5517/ccdc.csd.cc22276m.
[27] Range of distances according to a search at the Cambridge Crystallographic Data Centre database (updated November 2021) on phosphines PR3 (R= alkyl, aryl) coordinated to a Mn carbonyl fragment in turn bound to a second transition-metal atom. The search yielded 83 complexes, the largest subgroup displaying distances of ca. 2.29 ± 0.03Å, and only a dozen molecules displaying Mn−P distances below 2.25Å.
[28] A. Decken, M.A. Neil, F. Bottomley, Can. J. Chem. 79 (2001) 1321.
[29] The low-frequency bands for compounds **9e,f** actually are of energy comparable to the C−O stretches of the bridging carbonyls in the related phosphinidene-bridged homometallic complexes [Fe_2Cp_2(μ-PR*)(μ-CO)$(CO)_2$] (1769 cm^{-1}) and [$Ru_2Cp^*_2$(μ-PPh)(μ-CO)$(CO)_2$] (1757 cm^{-1}). See:
[a] M.A. Alvarez, M.E. García, R. González, A. Ramos, M.A. Ruiz, Organometallics 30 (2011) 1102.
[b] S. Takemoto, Y. Kimura, K. Kamikawa, H. Matsuzaka, Organometallics 27 (2008) 1780.
[30] R.H. Crabtree, M. Lavin, Inorg. Chem. 25 (1986) 805.
[31] M.L. Man, Z. Zhou, S.M. Ng, C.P. Lau, Dalton Trans. (2003) 3727.
[32] A search at the Cambridge Crystallographic Data Centre database (updated November 2021) on phosphines PR3 (R = alkyl, aryl) coordinated to a Ru carbonyl fragment in turn bound to a second transition-metal atom yielded some 1230 complexes, with Ru−P distances in the range 2.23-2.50Å, most of them around ca. 2.33 ± 0.05Å. There were more than one hundred examples with distances below 2.29Å.
[33] A search at the Cambridge Crystallographic Data Centre database (updated November 2021) on phosphines PR3 (R= alkyl, aryl) coordinated to a Fe carbonyl fragment in turn bound to a second transition-metal atom yielded some 1200 complexes, with Fe−P distances in the range 2.15-2.33Å, most of them around ca. 2.23 ± 0.04Å. There were a dozen examples with distances below 2.17Å.
[34] [a] M.E. García, V. Riera, M.A. Ruiz, D. Sáez, J. Vaissermann, J.C. Jeffery, J. Am. Chem. Soc. 124 (2002) 14304; [b] I. Amor, M.E. García, M.A. Ruiz, D. Sáez, H. Hamidov, J.C. Jeffery, Organometallics 25 (2006) 4857.
[35] M.E. García, D. García-Vivó, M.A. Ruiz, D. Sáez, Organometallics 36 (2017) 1756.
[36] M.A. Alvarez, M.E. García, D. García-Vivó, E. Huergo, M.A. Ruiz, Inorg. Chem. 57 (2018) 912.
[37] [a] A.D. Horton, M.J. Mays, P.R. Raithby, J. Chem. Soc., Chem. Commun. (1985) 247; [b] H.-J. Haupt, U. Flörke, G. Disse, C. Heinekamp, Chem. Ber. 124 (1991) 2191; [c] M.J. Mays, S.M. Owen, P.R. Raithby, P.F. Reinisch, G.P. Shields, G.A. Solan, J. Organomet. Chem. 528 (1997) 123.
[38] [a] C.J. Cramer, Essentials of Computational Chemistry, 2nd Ed., Wiley, Chichester, UK, 2004; [b] W. Koch, M.C. Holthausen, A Chemistś Guide to Density Functional Theory, 2nd Ed., Wiley-VCH, Weinheim, 2002.
[39] L. Yu, G.N. Srinivas, M. Schwartz, J. Mol. Struct. (Theochem) 625 (2003) 215.
[40] Two-bond couplings involving P atoms ($^2J_{PX}$) in metal complexes increase algebraically with P−M−X angle, and therefore are quite sensitive to the relative positioning of P and X. Their absolute values for piano-stool complexes of type $MCpPXL_2$ usually follow the order $|^2J_{cis}| > |^2J_{trans}|$. See, for instance, reference 19, and also B. Wrackmeyer, H.G. Alt, H.E. Maisel, J. Organomet. Chem. 399 (1990) 125.
[41] W.L.F. Armarego, C. Chai, Purification of Laboratory Chemicals, 7th ed., Butterworth-Heinemann, Oxford, U. K., 2012.
[42] A.R. Manning, P. Hacket, R. Birdwhistell, P. Soye, Inorg. Synth. 28 (1990) 148.
[43] [a] R.B. King, F.G.A. Stone, Inorg. Synth. 7 (1963) 110; [b] R.J. Haines, A.L.Du Preez, J. Chem. Soc., Dalton Trans. (1972) 944.
[44] P. Braunstein, H. Lehner, D. Matt, Inorg. Synth. 27 (1990) 218.
[45] R.B. King, Organometallic Synthesis, in: Transition Metal Complexes, 1, Academic Press, London, U. K., 1965, p. 158.
[46] W.F. Edgel, J. Lyford IV, Inorg. Chem. 9 (1970) 1932.
[47] , CrysAlis Pro, Oxford Diffraction Limited, Ltd., Oxford, U. K., 2006.
[48] L.J. Farrugia, J. Appl. Crystallogr. 32 (1999) 837.
[49] [a] G.M. Sheldrick, SHELXL2018, University of Gottingen, Germany, 2018; [b] G.M. Sheldrick, 2015 Acta Crystallogr. Sect. C, 71 5; [c] G.M. Sheldrick, 2008 Acta Crystallogr. Sect. A, 64 112.
[50] APEX3 v2019.11-0, Bruker AXS Inc., Madison (WI), USA, 2019.
[51] SAINT v8.40B, Bruker AXS Inc., Madison (WI), USA, 2018.
[52] L. Krause, R. Herbst-Irmer, G.M. Sheldrick, D. Stalke, J. Appl. Cryst. 48 (2015) 3.
[53] M.J. Frisch, G.W. Trucks, H.B. Schlegel, G.E. Scuseria, M.A. Robb, J.R. Cheeseman, G. Scalmani, V. Barone, G.A. Petersson, H. Nakatsuji, X. Li, M. Caricato, A.V. Marenich, J. Bloino, B.G. Janesko, R. Gomperts, B. Mennucci, H.P. Hratchian, J.V. Ortiz, A.F. Izmaylov, J.L. Sonnenberg, D. Williams-Young, F. Ding, F. Lipparini, F. Egidi, J. Goings, B. Peng, A. Petrone, T. Henderson, D. Ranasinghe, V.G. Zakrzewski, J. Gao, N. Rega, G. Zheng, W. Liang, M. Hada, M. Ehara, K. Toyota, R. Fukuda, J. Hasegawa, M. Ishida, T. Nakajima, Y. Honda, O. Kitao, H. Nakai, T. Vreven, K. Throssell, J.A. Montgomery Jr., J.E. Peralta, F. Ogliaro, M.J. Bearpark, J.J. Heyd, E.N. Brothers, K.N. Kudin, V.N. Staroverov, T.A. Keith, R. Kobayashi, J. Normand, K. Raghavachari, A.P. Rendell, J.C. Burant, S.S. Iyengar, J. Tomasi, M. Cossi, J.M. Millam, M. Klene, C. Adamo, R. Cammi, J.W. Ochterski, R.L. Martin, K. Morokuma, O. Farkas, J.B. Foresman, D.J. Fox, Gaussian 16, Revision A.03, Gaussian, Inc., Wallingford CT, USA, 2016.
[54] Y. Zhao, D.G. Truhlar, J. Chem. Phys. 125 (2006) 194101 1.
[55] S. Grimme, J. Antony, S. Ehrlich, H. Krieg, J. Chem. Phys. 132 (2010) 154104.
[56] P.J. Hay, W.R. Wadt, J. Chem. Phys. 82 (1985) 299.
[57] a)T.H. Dunning Jr., J. Chem. Phys. 90(1989) 1007.; [b] R.A. Kendall, T.H. Dunning Jr., R.J. Harrison, J. Chem. Phys. 96 (1992) 6796; [c] D.E. Woon, T.H. Dunning Jr., J. Chem. Phys. 98 (1993) 1358; [d] K.A. Peterson, D.E. Woon, T.H. Dunning Jr., J. Chem. Phys. 100 (1994) 7410; [e] E.R. Davidson, Chem. Phys. Lett. 260 (1996) 514.